Using Gene Knockouts to Identify the Roles of *dlx* Paralogs

Rainer Overman

Thesis submitted to the University of Ottawa in partial fulfillment of the requirements for the Master's degree in Biology

Department of Biology

Faculty of Science

University of Ottawa

Acknowledgements

I would first like to express my deepest gratitude to my supervisor, Marc Ekker, for his guidance, mentorship, and unwavering support throughout my graduate studies. Beyond teaching me how to think and work as a researcher, Marc is also an exceptional educator whose patience, insight, and encouragement have profoundly shaped my development both scientifically and personally. His commitment to student growth created an environment in which I was able to learn and grow with confidence, and I aspire to one day be as good of a teacher as he is a professor.

I would also like to thank the members of the laboratory who made this work possible and made the lab an engaging and enjoyable place to work. In particular, I am grateful to Vishal Saxena for his invaluable help troubleshooting experiments and for always being willing to share his expertise and advice. I would also like to thank Gabrielle Queneville and Zachary Villeneuve for the many stimulating conversations, scientific discussions, and moments of camaraderie that made days in the lab far more rewarding.

Special thanks are also owed to my honours students, Maika Harvey and Emma Diniz, whose assistance with experiments contributed greatly to this work. Their enthusiasm and dedication were sincerely appreciated.

Finally, I would like to thank my cat, Smudge, for providing constant companionship, comfort, and many much-needed cuddles throughout the writing of this thesis. Her presence made even the most stressful writing sessions a little easier.

Statement of contributions

The experiments presented in this thesis were executed by myself. However certain contributions should be noted. Gabrielle Queneville, Maika Harvey, and Emma Diniz undergraduate students assisted with some of the results in chapters 3.1.

Abstract

The dlx gene family plays a critical role in the development of GABAergic interneurons and is uniquely organized into conserved bigene clusters regulated by shared intergenic enhancers. Although the dlx genes have been extensively studied, the functional significance of this genomic organization and the individual contributions of specific paralogs to interneuron subtype specification remain incompletely understood. This study investigated the effects of dlx gene deletions on GABAergic interneuron populations in the zebrafish brain and developed optimized quantitative PCR (qPCR) primers to facilitate future transcriptional analyses of this gene family.

Immunohistochemical analyses were performed to evaluate the effects of dlx deletions on parvalbumin (PV)-, somatostatin (SST)-, and calretinin (CR)-expressing interneuron populations. In parallel, qPCR primers were designed and optimized for the highly conserved dlx gene family to support future studies of gene expression and regulatory interactions.

PV immunostaining exhibited substantial variability, preventing reliable quantitative analysis. In contrast, consistent results were obtained for SST and CR populations. Deletion of dlx1a and dlx5a resulted in marked reductions in SST-expressing neurons, indicating that these genes play key roles in SST interneuron development. Similarly, dlx2a and dlx5a were found to contribute significantly to the development of CR-expressing neurons. The optimized qPCR primers provide a robust methodological resource for future investigations of transcriptional regulation within dlx gene clusters.

These findings demonstrate distinct roles for individual dlx paralogs in the specification of GABAergic interneuron subtypes while providing new molecular tools for studying dlx gene regulation. By integrating histological and molecular approaches, this work advances our understanding of the regulatory architecture and functional significance of dlx gene organization and establishes a foundation for future investigations into the mechanisms underlying GABAergic brain development.

Table of Contents

List of Figures

List of Tables

List of Abbreviations

bp	base pairs
BSA	bovine serum albumin
cDNA	complementary DNA
CGE	caudal ganglionic eminence
CNS	central nervous system
CR	calretinin
DAPI	4’,6-diamidino-2-phenylindole
ddPCR	digital droplet PCR
DEPC	diethyl pyrocarbonate
Dll	distal-less
Dlx	distal-less homeobox
DMSO	dimethyl sulfoxide
DNA	deoxyribonucleic acid
FISH	fluorescent in situ hybridization
GABA	gamma-aminobutyric acid
Gad1	glutamate decarboxylase 1
Gad2	glutamate decarboxylase 2
gDNA	genomic DNA
hpf	hours post fertilization
HTH	helix–turn–helix
IHC	immunohistochemistry
KO	knockout
LGE	lateral ganglionic eminence
MGE	medial ganglionic eminence

mRNA	messenger RNA
OCT	optimal cutting temperature
PBS	phosphate-buffered saline
PBS-DT	phosphate-buffered saline with detergent solution
PBSTx	phosphate-buffered saline with Triton X
PCR	polymerase chain reaction
PFA	paraformaldehyde
PPa	anterior parvocellular preoptic nucleus
PPp	posterior parvocellular preoptic nucleus
PV	parvalbumin
qPCR	quantitative polymerase chain reaction
qRT-PCR	quantitative reverse transcription PCR
RNA	ribonucleic acid
RPM	revolutions per minute
SEM	standard error of the mean
sgRNA	single-guide RNA
SST	somatostatin
SSC	saline-sodium citrate
SVZ	subventricular zone
TBST	Tris-buffered saline with Tween
TeO	optic tectum
TNT	Tris-NaCl-Tween buffer
VIP	vasoactive intestinal peptide
VZ	ventricular zone
WT	wild type

1. Introduction

1.1 General Introduction

The *distal less homeobox* gene family comprises a group of highly conserved homeobox transcription factors that play essential roles in vertebrate embryonic development, particularly in the formation of the forebrain and the specification of GABAergic interneurons. In vertebrates, *dlx* genes are uniquely organized into convergently transcribed bigene clusters regulated by shared intergenic enhancers, suggesting a complex regulatory architecture that has been evolutionarily conserved. Although their importance in neural development is well established, many aspects of their individual functions and genomic organization remain poorly understood.

This thesis focuses on the *dlx* gene family, with particular emphasis on aspects of its function and genomic organization that remain incompletely understood. The first objective is to investigate the role of *dlx* genes in brain development, specifically in the specification and maturation of GABAergic interneurons. This work aims to refine our understanding of how individual *dlx* paralogs contribute to the development of distinct interneuron subpopulations, addressing the extent to which their functions are redundant or specialized. By examining gene-specific effects, this objective seeks to clarify the precise regulatory roles of *dlx* genes in establishing inhibitory neuronal diversity.

The second objective addresses the unusual genomic organization of the *dlx* gene family. *dlx* genes are arranged in convergently transcribed bigene clusters, a rare configuration in vertebrate genomes, the functional significance of which remains largely unknown. To investigate this, this thesis aims to design and validate quantitative PCR primers targeting individual *dlx* genes, enabling precise measurement of their transcriptional activity. These tools could one day be used to assess the regulatory influence of intergenic enhancers and to examine potential cross-regulatory interactions between paired *dlx* genes within each cluster. Together, these objectives seek to advance our understanding of both the functional roles and regulatory architecture of the *dlx* gene family in vertebrate neurodevelopment.

1.1 *Dlx* genes and their organization

Dlx genes encode a group of homeobox-containing transcription factors that are found in vertebrates. These genes are known to be essential in embryonic development, particularly in the development of the craniofacial region and sensory organs. (Depew et al., 1999) . *Dlx* genes encode proteins that contain a highly conserved DNA-binding domain, the homeodomain, which enables them to bind to specific target genes to regulate their expression (Morasso & Radoja, 2005) . *Dlx* genes are closely related to the *distal-less* (*dll*) gene found in fruit flies, which is involved in the development of distal appendages and peripheral nervous system. The conservation of these genes throughout evolution indicates that these genes are essential regulators in development (Panganiban & Rubenstein, 2002)(Panganiban & Rubenstein, 2002).

1.1.1 Evolutionary origin of the *Dlx* gene family

The *Dlx* gene family is widely recognized to have originated through duplication events of the ancestral *Distal-less* (*dll*) gene, which was first identified in the fruit fly *Drosophila melanogaster*. In invertebrates, *dll* plays a critical role in limb formation and the patterning of multiple appendage-related structures, highlighting its function as a key developmental regulator (Panganiban et al., 1997). The evolutionary relationship between *dll* and vertebrate *Dlx* genes is supported by the presence of a highly conserved DNA-binding homeodomain, composed of three α-helices arranged in a helix–turn–helix (HTH) motif, which enables these transcription factors to regulate a broad array of downstream target genes. During early vertebrate evolution, the ancestral *dll* gene is thought to have undergone an initial duplication event, giving rise to the first *Dlx* bigene cluster. Subsequent duplication events—likely associated with whole-genome duplications—produced three conserved *Dlx* bigene clusters (*Dlx 1/2*, *Dlx 3/4*, and *Dlx 5/6*), an organization that is maintained across all extant vertebrates (Fig. 1) (Stock et al., 1996; Zerucha & Ekker, 2011). Further evidence supporting this evolutionary origin is reflected in the sequence similarities observed among individual *Dlx* genes, with *Dlx1*, *Dlx6*, and *Dlx4* exhibiting greater similarity to one another than to their respective bigene partners. It is widely accepted that *Dlx1*, *Dlx6*, and *Dlx4* arose from duplication of a common ancestral *dlx* gene, a pattern that is likewise observed for *Dlx2*, *Dlx5*, and *Dlx3* (Ghanem et al., 2003).

In teleost fish, including zebrafish, an additional genome-wide duplication event further expanded the *dlx* gene repertoire, resulting in the formation of extra bigene clusters (Taylor et al., 2003) . Over evolutionary time, however, these duplicated clusters experienced gene loss, leading to the retention of the unpaired *dlx* genes *dlx4a* and *dlx2b* in the zebrafish genome. Despite decades of investigation, the functional significance of the conserved *Dlx* bigene cluster organization remains poorly understood. The remarkable conservation of this atypical genomic arrangement across vertebrate species suggests strong selective pressure to preserve it. This organization is widely hypothesized to facilitate coordinated gene regulation through shared cis-regulatory elements located within intergenic regions; however, the precise mechanisms by which these elements influence *Dlx* gene expression and function remain an active area of research (Ghanem et al., 2003a) .

Although *Dlx* proteins retain the core DNA-binding function of their *dll* ancestor, the vertebrate *Dlx* gene family has undergone substantial functional diversification. Beyond roles in limb and appendage development, *Dlx* genes are now known to be essential for craniofacial patterning, sensory organ formation, and, critically, multiple aspects of central nervous system development, including forebrain patterning and interneuron differentiation (Merlo et al., 2000).

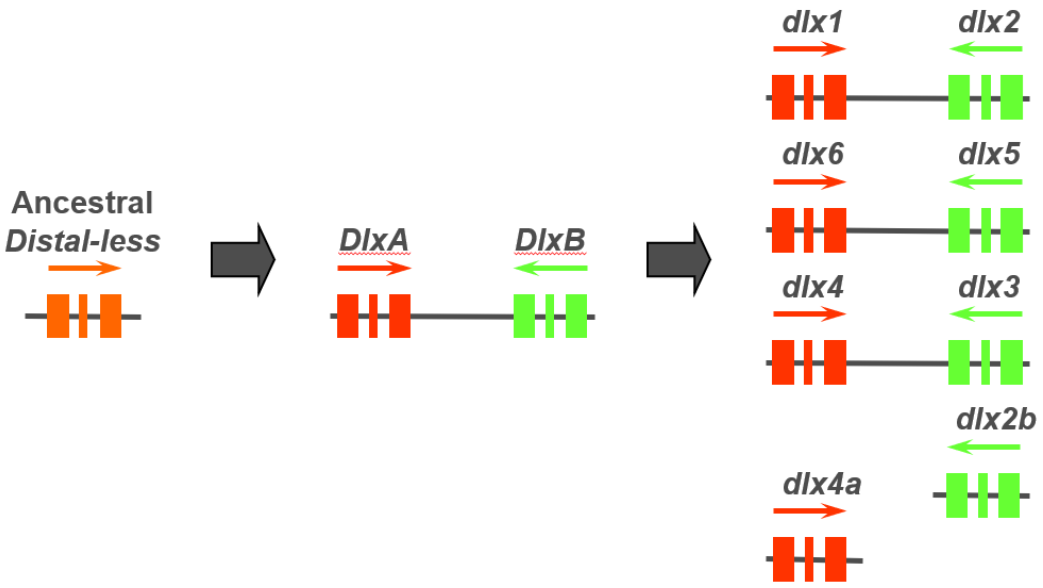

Figure 1. Schematic illustration of the evolution of the *Dlx* gene family in zebrafish. The *dlx* gene family is derived from the ancestral *Distal-less* (*dll*) gene. An initial gene duplication event in early vertebrate evolution gave rise to a bigene cluster (labeled *DlxA* and *DlxB* in this figure) arranged in a convergent (tail-to-tail) orientation. Subsequent duplication events generated three conserved *dlx* bigene clusters: *dlx1/2*, *dlx5/6*, and *dlx3/4*. In teleosts such as zebrafish, an additional genome duplication further expanded the *dlx* family, resulting in duplicated clusters and the creation of *dlx2b* and *dlx4a*. Over evolutionary time, *dlx2b and dlx4a* lost their corresponding pairs, leading to the presence of both paired and unpaired *dlx* genes in the zebrafish genome. Arrows indicate gene orientation, and colored to illustrate the ancestral *dlx* gene from which they arose.

1.1.2 Genomic organization of the Dlx gene family

The *Dlx* gene family exhibits a distinctive and evolutionarily conserved genomic organization characterized by the presence of convergently transcribed bigene clusters. In vertebrates, the six *Dlx* genes are arranged into three paired clusters—*Dlx1/2*, *Dlx3/4*, and *Dlx5/6*—in which each gene pair is positioned in a tail-to-tail orientation and separated by relatively small intergenic regions (Figure 2). This clustered configuration is conserved across vertebrate species, indicating strong selective pressure to maintain this genomic architecture (Ellies et al., 1997) . These intergenic regions harbor shared cis-regulatory elements capable of coordinating the spatial and temporal expression of both genes within a cluster (Ghanem et al., 2003a) . Such shared regulatory control is thought to underlie the partially overlapping expression domains and functional redundancy observed among paired *Dlx* genes during development. Despite this progress, the precise regulatory logic governing how individual enhancers selectively modulate one or both genes within a cluster remains poorly understood. The persistence of this unusual bigene arrangement across hundreds of millions of years of vertebrate evolution suggests that clustered organization is integral to *Dlx* gene function, rather than a neutral byproduct of duplication events.

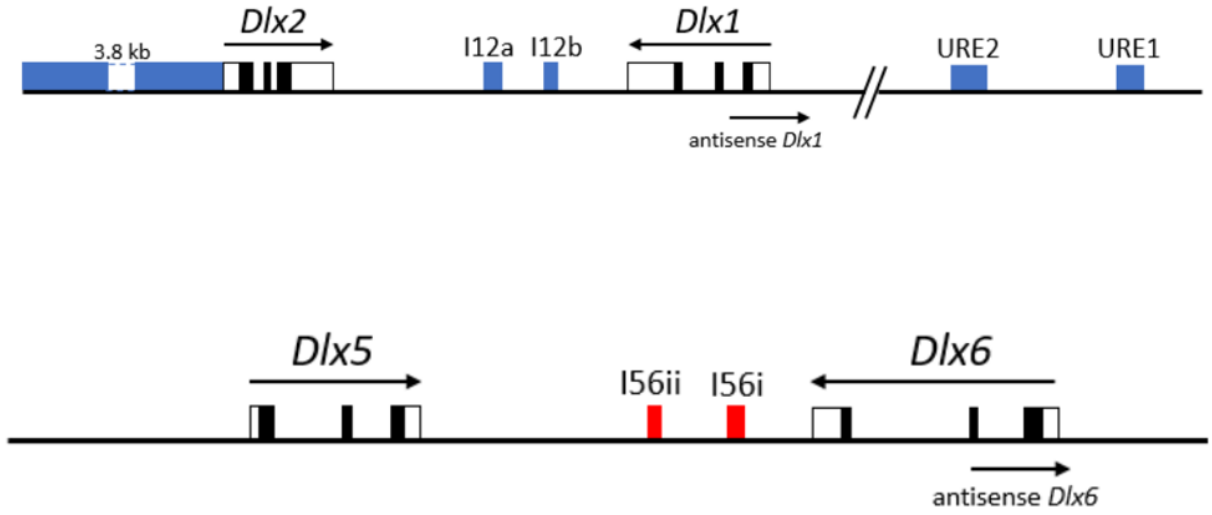

Figure 2. Organization of *Dlx* genes in mice. Only the *Dlx* genes expressed in the brain our shown here. The direction of transcription is indicated by arrows. Regulatory elements are symbolized with colored boxes. Figure modified from Rubenstein et al. 2024

1.1.3 Dlx genes involvement in neural development

It has long been established that the *Dlx* gene family plays a crucial role in neural development, particularly in the specification and maturation of GABAergic interneurons. Members of the *Dlx* family are highly expressed in the medial, lateral, and caudal ganglionic eminences of the developing forebrain, where they regulate the migration and differentiation of GABAergic neuronal precursors (Liu, n.d.) . During brain development, neurons originate in a region known as the proliferative zone and subsequently undergo two distinct phases of migration: tangential and radial migration (Figure 3). Tangential migration refers to movement parallel to the surface of the brain, whereas radial migration occurs perpendicular to it. These two phases occur sequentially, with tangential migration preceding radial migration, although the mechanisms that trigger this transition require more research.

The involvement of *Dlx* genes in GABAergic neuron specification has been extensively demonstrated in mouse models. Within the proliferative zone, *Dlx* genes are expressed in a tightly regulated spatiotemporal pattern that corresponds to distinct stages of interneuron development. Expression of *Dlx2* occurs first, followed closely by *Dlx1*, with both genes showing strong expression in the ventricular zone (VZ) and subventricular zone (SVZ). This expression pattern coincides with the initiation of migration in newly generated GABAergic interneuron precursors. As these precursor neurons begin migrating and exit the VZ and SVZ, expression of *Dlx5* and *Dlx6* becomes more prominent. In contrast to *Dlx1* and *Dlx2*, these genes show reduced expression within the VZ and SVZ—*Dlx6*, in particular, is largely absent from the VZ—but display strong expression in migrating interneurons and in the developing cortex (Wonders

& Anderson, 2006) (Figure 3). This shift in gene expression corresponds with later stages of interneuron migration and continued differentiation of GABAergic precursors.

Our understanding *of* dlx impact on GABAergic neurons have been made evident through the use of loss-of-function studies in mice that demonstrated that *Dlx* genes are central regulators of forebrain development, with particularly critical roles in the generation, migration, and maturation of GABAergic interneurons originating in the subpallium. While single *Dlx* gene knockouts often produce subtle phenotypes due to compensatory activity among paralogs, compound mutants reveal the full extent of their function (Rubenstein et al., 2024) . In *Dlx1/2* double knockout mice result in severe impairment in the tangential migration of interneuron precursors from the medial and lateral ganglionic eminences to the developing neocortex, hippocampus, and olfactory bulb (Anderson et al., 1997; Long et al., 2007) . As a result, there is a dramatic depletion of cortical and olfactory bulb GABAergic interneurons, accompanied by a corresponding accumulation of immature progenitors within the subpallium. These cells often fail to properly exit the cell cycle, downregulate progenitor markers, or upregulate genes required for migration, indicating that *Dlx1/2* function is required both for initiating differentiation and enabling migratory competence.

At the molecular level, *Dlx1/2* mutants show reduced expression of key downstream targets involved in interneuron development, including genes regulating cytoskeletal dynamics, guidance cues, and neurotransmitter synthesis such as *Gad1* and *Gad2* (Le et al., 2017; Long et al., 2009) . *Dlx1/*2 loss of function leads not only to fewer interneurons reaching their cortical destinations, but also to deficits in their maturation into fully functional inhibitory neurons. In

Dlx5/6 double mutants, defects are somewhat later in onset and include impairments in interneuron subtype specification, suggesting a role for these genes in refining interneuron identity and connectivity after migration (Cho et al., 2015; MacKenzie et al., 2019)

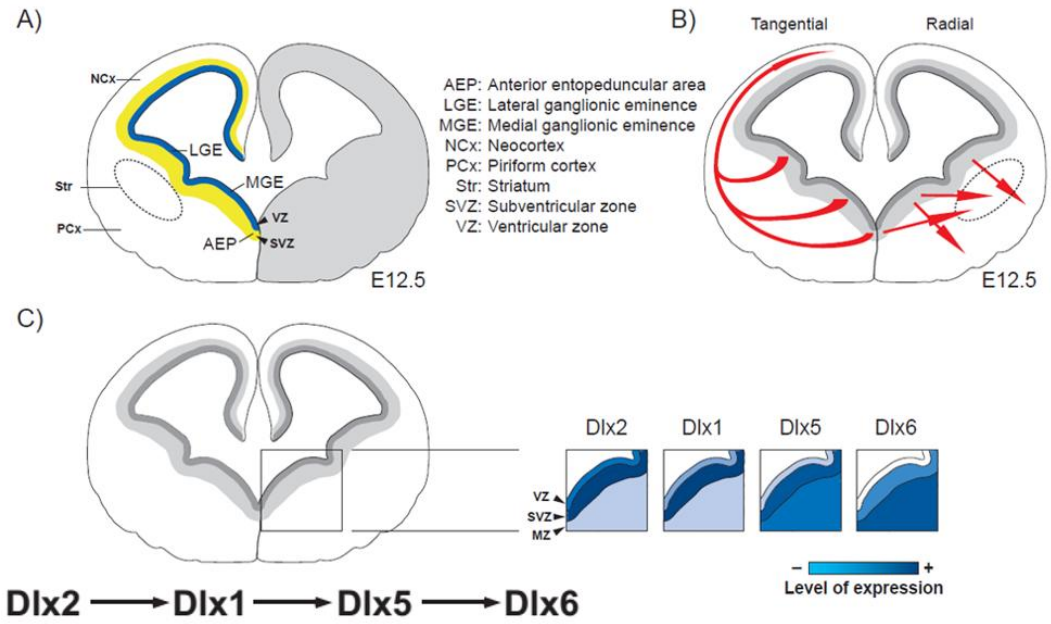

Figure 3. Role of *Dlx* genes in GABAergic interneuron migration during development in mice. A) Schematic of of embryonic mouse telencephalon at E12.5 highlighting the MGE and LGE the primary sites of GABAergic interneuron production. Also highlited are the VZ and SVZ the proliferative region from which neuron progenitors first develop. B) Schematic of embryonic mouse telencephalon illustrating the two phases of migration that all progenitor neurons undergo. C) Spatiotemporal expression patterns of *Dlx* genes during interneuron development, illustrating the sequential activation of *Dlx2*, *Dlx1*, *Dlx5*, and *Dlx6*. Early expression of *Dlx2* and *Dlx1* is found in the VZ and SVZ and is associated with the initiation of interneuron migration, whereas *Dlx5* and *Dlx6* expression predominates in migrating cells within the cortex, corresponding to later stages of migration and differentiation. Color intensity reflects relative gene expression levels. Together, these patterns highlight the coordinated role of *Dlx* genes in regulating the generation, migration, and maturation of GABAergic interneurons. (Marc Ekker Unpublished)

balance between excitation and inhibition within neural networks (Tremblay et al., 2016).

During development, most cortical GABAergic interneurons originate from progenitor regions of the ventral telencephalon, specifically the medial, lateral, and caudal ganglionic eminences (Figure 3A), before undergoing tangential migration into the cortex where they integrate into local neuronal circuits (Wonders & Anderson, 2006) . Interestingly, during early stages of neural development GABA signaling is excitatory rather than inhibitory due to immature intracellular chloride gradients in developing neurons. As neural circuits mature and ionic gradients are established, GABA gradually assumes its canonical inhibitory role within the central nervous system (Ganguly et al., 2001) .

GABAergic interneurons are highly heterogeneous and can be classified into multiple subclasses based on molecular markers, morphology, electrophysiological properties, and connectivity patterns. For the purposes of this work, classification will primarily rely on molecular markers. Using this framework, cortical GABAergic interneurons are commonly divided into three major subclasses: parvalbumin (PV), somatostatin (SST), and calretinin (CR) interneurons. Together, these three groups account for the vast majority (up to 95%) of cortical inhibitory interneurons, with PV interneurons representing the largest proportion (Rudy et al., 2011) . Although these molecular markers are frequently used to define interneuron subclasses, it is important to note that interneuron identity can be complex, and some neurons may exhibit overlapping molecular characteristics.

1.2.1 PV neurons

Parvalbumin-expressing (PV) interneurons represent one of the most abundant and functionally important subclasses of cortical GABAergic interneurons. These neurons are characterized by their fast-spiking electrophysiological properties, high expression of the calcium-binding protein parvalbumin, and their ability to generate rapid, precisely timed inhibitory signals within cortical circuits (Hu et al., n.d.). Two principal morphological subtypes of PV interneurons have been identified: basket cells and chandelier cells. Basket cells form synapses around the soma and proximal dendrites of pyramidal neurons, whereas chandelier cells uniquely target the axon initial segment, the site where action potentials are initiated (Klausberger & Somogyi, 2008). Through these connections, PV interneurons exert strong perisomatic inhibition that allows them to tightly regulate the firing output of excitatory pyramidal neurons and synchronize neuronal activity across local circuits (Pouille & Scanziani, 2001). Functionally, PV interneurons play a crucial role in the generation and maintenance of gamma-frequency oscillations (30–80 Hz), which are associated with cognitive processes such as attention, sensory processing, and working memory (Bartos et al., 2002)(Bartos et al., 2002). Developmentally, PV interneurons originate primarily from progenitor populations in the medial ganglionic eminence (MGE) of the embryonic ventral telencephalon (Wonders & Anderson, 2006). These progenitors give rise to interneuron precursors that migrate tangentially into the developing cortex before switching to radial migration to reach their final laminar positions. The maturation of PV interneurons occurs relatively late in cortical development and is accompanied by the acquisition of fast-spiking properties and the formation of perisomatic synaptic contacts.

Due to their critical role in maintaining the balance between excitation and inhibition in cortical networks, dysfunction of PV interneurons has been implicated in several neurological and psychiatric disorders, including epilepsy, schizophrenia, and autism spectrum disorders(Marín, 2012)

PV neurons are among the most consistently affected populations in *Dlx* knockout mouse models. Loss of *Dlx1/2* disrupts the migration and maturation of MGE-derived interneurons, from which PV cells originate. As a result, PV interneuron numbers are significantly reduced in the cortex and hippocampus, and those that do develop often show impaired maturation and synaptic integration. These deficits are associated with altered inhibitory circuit function and have been linked to epilepsy-like phenotypes observed in *Dlx* mutants (Anderson et al., 1997b; Cobos et al., 2005a; Pla et al., 2017).

1.2.2 SST neurons

Somatostatin-expressing (SST) interneurons constitute another major class of cortical inhibitory neurons and are distinguished by their role in modulating dendritic activity and synaptic integration within pyramidal neurons. These interneurons express the neuropeptide somatostatin and display a wide range of morphological and electrophysiological properties, reflecting the diversity within this population (Urban-Ciecko & Barth, 2016). One of the most well-studied SST interneuron subtypes is the Martinotti cell, which is characterized by axonal projections that extend toward the superficial layers of the cortex, particularly layer I, the outermost layer of the neocortex. In this region, Martinotti cells form inhibitory synapses on the

distal apical dendrites of pyramidal neurons, allowing them to regulate the integration of excitatory inputs arriving from corticocortical and thalamocortical projections(Y. Wang et al., 2004). Through this dendrite-targeting inhibition, SST interneurons act as key modulators of synaptic plasticity and signal integration, shaping how excitatory neurons respond to incoming stimuli. SST interneurons also participate in complex inhibitory circuits involving other interneuron populations, including disinhibitory interactions with PV interneurons and vasoactive intestinal peptide (VIP)-expressing interneurons (Lee et al., 2013; Pfeffer et al., 2013). Developmentally, SST interneurons arise predominantly from progenitors within the medial ganglionic eminence, similar to PV interneurons, although their differentiation is regulated by distinct transcriptional programs. After their generation, SST interneuron precursors migrate tangentially into the cortex and subsequently integrate into local circuits where they contribute to the regulation of cortical excitability and sensory processing (Wonders & Anderson, 2006). The functional role of SST interneurons in dendritic inhibition makes them particularly important for controlling the gain of cortical responses and maintaining excitation–inhibition balance within neural networks

SST neurons, which are also derived from the MGE, are similarly impacted by *Dlx* gene disruption, although in some cases to a lesser extent than PV populations. In *Dlx1/2* knockout mice, SST interneurons exhibit defective tangential migration to the cortex, leading to reduced cortical density. Additionally, *Dlx1* has been shown to be important for the survival of a subset of SST interneurons postnatally, with mutant mice displaying progressive loss of these cells over time. This reduction contributes to an imbalance in inhibitory signaling and further exacerbates network dysfunction (Anderson et al., 1997b; Cobos et al., 2005).

1.2.3 CR neurons

Calretinin-expressing (CR) interneurons represent a distinct subclass of cortical inhibitory neurons that differ from PV and SST interneurons in both their developmental origin and their functional roles within cortical circuits. These interneurons are characterized by the expression of the calcium-binding protein calretinin and exhibit diverse morphologies and electrophysiological properties. Unlike PV and SST interneurons, which originate primarily from the medial ganglionic eminence, CR interneurons are largely derived from progenitor populations located in the CGE of the embryonic ventral telencephalon (Wonders & Anderson, 2006). Following their generation, CR interneuron precursors migrate tangentially into the developing cortex, where they preferentially populate the superficial cortical layers, particularly layers II and III. Functionally, CR interneurons frequently form synaptic connections with other interneurons rather than directly targeting excitatory pyramidal neurons. Through these connections, they contribute to disinhibitory circuits, in which inhibition of other inhibitory neurons results in a net increase in excitatory neuronal activity (Cauli et al., 2014; Gulyás et al., 1996). This form of circuit modulation is thought to provide flexible control over cortical network dynamics and facilitate context-dependent information processing. CR interneurons are also implicated in the coordination of local inhibitory networks and may contribute to the synchronization of neuronal populations across cortical microcircuits. Due to their involvement in interneuron–interneuron communication and network modulation, CR interneurons play an important role in shaping cortical information flow and maintaining functional circuit balance. Alterations in the development or function of these neurons have been linked to disruptions in

cortical circuitry associated with neurodevelopmental disorders (Vanessa Becerra-Hernández et al., 2025).

CR which are largely derived from the CGE and not the MGE, are also affected in *Dlx* mutants, though their dependence on *Dlx* genes differs somewhat from MGE-derived populations. Studies have shown that *Dlx1* in particular plays a key role in the differentiation and survival of CR interneurons. In *Dlx1* knockout mice, CR-positive interneurons initially develop but undergo increased apoptosis during postnatal stages, leading to a marked reduction in their numbers in the adult cortex. This highlights a role for *Dlx* genes not only in early development but also in maintaining interneuron populations (Cobos et al., 2005a)

1.3 The zebrafish model

Zebrafish (*Danio rerio*) have emerged as a widely used model organism in biology due to numerous advantages they offer for scientific research. The rapid generation time and large number of externally developing embryos allow for easy manipulation and observation, making zebrafish ideal for large-scale experiments. Their small size and ease of maintenance further enhance their appeal as a model organism. Zebrafish embryos are transparent, which permits visualization of internal structures and processes, such as nervous system development (Briggs, 2002). In addition, the zebrafish genome is well understood and gene manipulation and editing have become relatively simple tasks. Zebrafish share numerous molecular and genetic pathways with humans, making them an invaluable tool for investigating human diseases and testing

potential therapies. 70% of human genes have been found to have a zebrafish ortholog making them a useful model for humans (Howe et al., 2013)

In addition to these general advantages, zebrafish represent a valuable model for studying neural development. A notable characteristic shared by zebrafish and other teleost fish is their remarkable capacity for continued brain growth and neurogenesis well into adulthood (Kizil et al., 2012). This ability allows researchers to investigate not only early neural development but also processes such as adult neurogenesis and brain regeneration, thereby expanding the range of experimental approaches available for studying nervous system development and repair. Although important anatomical and physiological differences exist between zebrafish and humans, many major brain regions and developmental pathways are conserved across these species (Burgess & Burton, 2023) (Fig. 4). This conservation enables meaningful comparisons to be drawn between zebrafish and mammalian systems, making zebrafish a powerful model for exploring the mechanisms underlying vertebrate brain development.

When it comes to research into GABAergic neurons more specifically, studies in zebrafish have demonstrated that many of the molecular mechanisms governing GABAergic neuron specification and differentiation are highly conserved with those observed in mammals. In particular, genes known to regulate interneuron development in mammals, including members of the *dlx* gene family, *gad65*, and *gad67* (genes involved in the production of GABA), show similar expression patterns in the zebrafish forebrain and other regions of the developing central nervous system (MacDonald et al., 2013; Ramaswamy et al., 2020). These genes are expressed in ventral telencephalic domains that are considered homologous to the mammalian ganglionic eminences, the primary sites of GABAergic interneuron production. Research in

zebrafish has therefore provided valuable insights into the genetic programs that control GABAergic neuron specification, migration, and differentiation during vertebrate brain development. Additionally, transgenic zebrafish lines expressing fluorescent reporters under the control of GABAergic markers have allowed detailed characterization of inhibitory neuronal populations and their developmental trajectories (Mendes et al., 2020a). Through these approaches, zebrafish have contributed significantly to the identification of regulatory networks and signaling pathways involved in the establishment of GABAergic circuits, further supporting the conservation of inhibitory neuron development across vertebrate species.

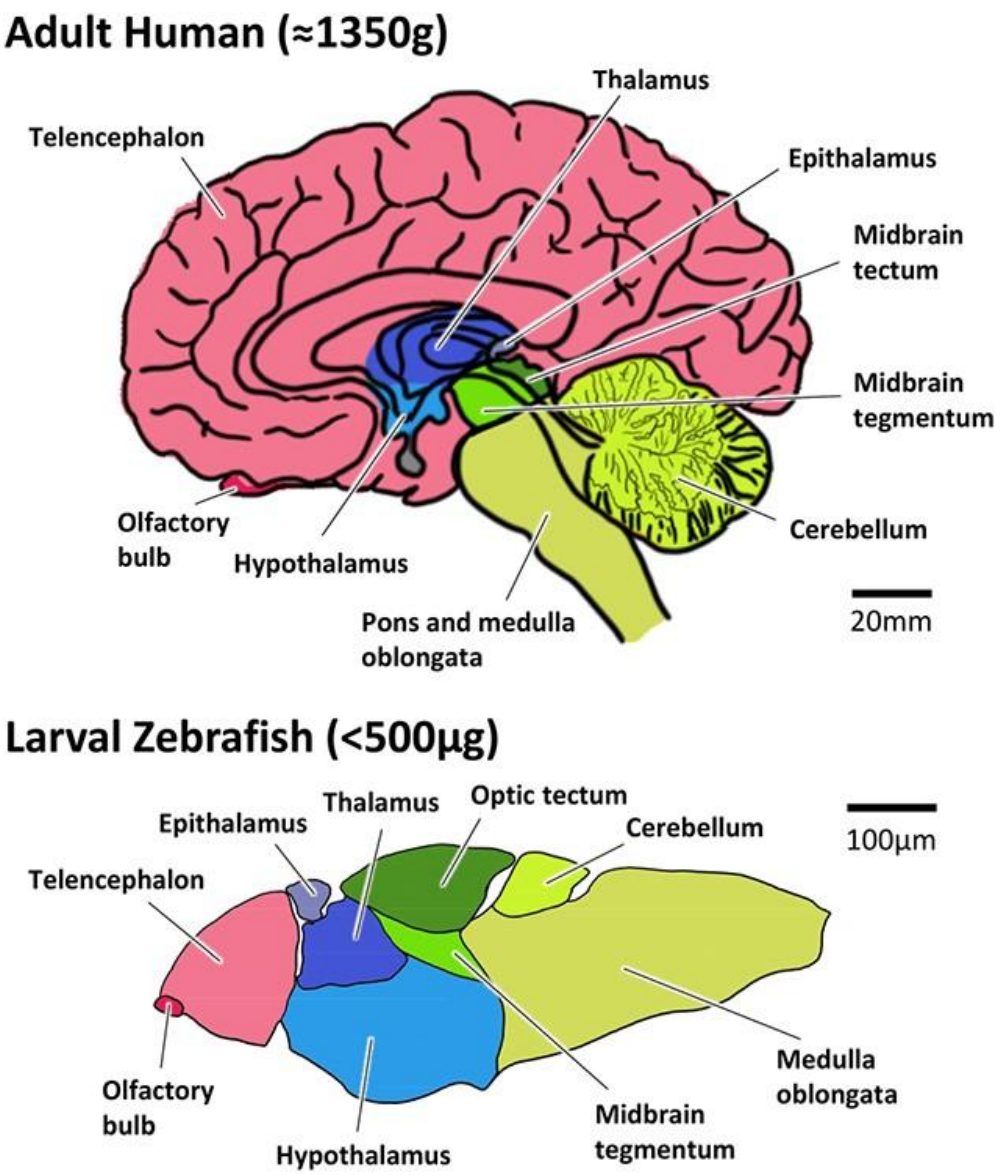

Figure 4. Conservation between Human and Zebrafish brain (Burgess and Burton 2023)

1.4 Statement of purpose and objective

Although the *dlx* gene family has long been studied there still remains major gaps in our understanding of both their organization as well as impact in brain development. When it comes to brain development even though it has been long established that the *dlx* genes are essential for GABAergic neuron development it is still unknown more specifically which gene is performing what and how. My first objective aims to tackle this issue by observing the impact of various KO zebrafish lines for *dlx* on the 3 major subpopulations of GABAergic neurons. Furthering our understanding of the development of GABAergic neurons could one day potentially lead to novel treatments for the wide swathe of various illnesses caused by their dysregulation (Guo et al., 2024).

When it comes to *dlx* organization even less is understood when it comes to their function. Although it is widely accepted that the organization of the *dlx* gene families in their distinctive bigene clusters must be important to some aspect of their functioning due to how well conserved this organization is across all species, it is still not understood what exactly this organization is providing. My second objective aims to further our understanding of this through the use of qPCR on various dlx KO models of zebrafish. qPCR represents a valuable approach for achieving this objective, as it enables precise measurement of transcript levels for individual *dlx* genes within our mutant models. This method allows for accurate quantification of how the loss of a single *dlx* gene, or disruption of its associated intergenic enhancers, influences the expression of other members of the gene family. For instance, applying qPCR to the *inter56* mutant line (a KO line of the *dlx5/6* intergenic enhancers) will provide, for the first time, a direct

assessment of how these intergenic regulatory elements contribute to the transcriptional regulation and coordination of *dlx* gene expression.

Objective 1: Further characterize the impact of the *dlx* gene family on neural development. We hypothesize that the *dlx* gene family is required for the proper development, differentiation, and/or survival of GABAergic interneurons during neural development. We predict that the loss of dlx genes will result in reduced number of key GABAergic neuron populations (SST, PV, CR)

Objective 2: Optimize functional qPCR primers for the *dlx* gene family. The *dlx* gene family presents unique challenges qPCR analysis due to factors related to their expression patterns and genomic organization. The objective of this work is to design and validate functional qPCR primers for these genes, which may serve as a resource for future studies within the laboratory on their organization. In parallel, existing RNA-seq datasets and bioinformatic approaches will be utilized as a proof of concept to demonstrate the types of analyses that can be performed to further investigate *dlx* gene expression and organization.

2. Materials and Methods

2.1 Fish Husbandry

All experiments described in this thesis were conducted in accordance with protocols approved by the Animal Care Committee at the University of Ottawa. Zebrafish were maintained at 28.5 °C under a controlled 14-hour light/10-hour dark cycle. All experiments performed where done on an even mix of male and female adult zebrafish aged between 4 and 16 months, with the exception of RNA extraction for qPCR which were performed on larvae (24-72 hpf). The various *dlx* mutant lines used for my experiments are described in Table 1. All lines are a complete deletion of the *dlx* gene from the 5'UTR or the first exon to the 3'UTR.

Adult zebrafish were genotyped by fin clipping. Fish were briefly anesthetized in 0.016% tricaine methane sulfonate, and a small portion of the caudal fin was removed using a sterile scalpel. Fin tissue was collected into individual microcentrifuge tubes for genomic DNA extraction. Following recovery in fresh system water, fish were returned to their home tanks and monitored until normal swimming behavior resumed. Genomic DNA was extracted from fin clip samples using a sodium hydroxide (NaOH) extraction protocol. Fin tissue was incubated in 50 mM NaOH at 95°C for 20 minutes to lyse cells and release genomic DNA. Samples were then cooled to room temperature and neutralized with 1 M Tris-HCl (pH 8.0). The resulting DNA lysate was briefly centrifuged to pellet debris and the supernatant was used directly as the template for polymerase chain reaction (PCR). PCR amplification was performed using allele-specific primers designed to distinguish wild-type and mutant alleles (Table 2).

Mutant Line	sgRNA 1	sgRNA 2
dlx1a	GGACCAATCAGAGAGCACCT	GGTCCCCTGAACTGGGCCAT
dlx2a	GGCAATGATCAACGTGGCAT	GGAAACGCTTTCGGCCCCTA
dlx5a	GGCTATTACAGCCCTGCCGG	GGCTCTCGATATAATGGCAT
dlx6a	GGGAGCCGGAATGGAGACAG	GGCGTGTCAATGGTCGACAA
dlx5i6	GGCGTGTCAATGGTCGACAA	GGCTCTCGATATAATGGCAT
inter56	GGGAGCCGGAATGGAGACAG	GGCAGGTACGGACTGTGGTG

Table 1. 5' to 3' sgRNA sequences used for generating the *dlx* mutant lines

Mutant Line	Primers	Expected Band Sizes
dlx1a	*dlx1a* F2: CCTCCCAAGTACGGCCTATG *dlx1a* R1: CAGCACATCTGGGCTACTCC *dlx1a* R3: GTGTTTCTTCTCCGGTGCGA	Wt : 787bp Mutant: 359bp
dlx2a	*dlx2a* F2: ATCTGGTTCCAGAATCGTCGT *dlx2a* R2: CAAGTCCCAGGAATCGCCG *dlx2a* R3: TCTGATTCACCCTGCTGCAA	Wt: 636bp Mutant: 414bp
dlx5a	*dlx5a* L1C: ATCAAGAACCAGGCGCATCT *dlx5a* R4A: GAGCCCACACAGAGATAGCA *dlx5a* R6A: CCCTTTTCAGCTCTCCACGAT	Wt: 498bp Mutant: 306bp
dlx6a	*dlx6a* L2: GGAGGCTCAAGACTCGTCAA *dlx6a* R2A: TTGCTGACATACGACGGGG *dlx6a* R3: AAAACGATTCGCTTCCTGTC	Wt: 429bp Mutant: 323bp
dlx5i6	Use *dlx6a* L2, *dlx6a* R2A, and *dlx5a* R6a for genotyping	Wt: 429bp Mutant: 200-230bp
inter56	*inter56* L2: AGCTACATGCCCGGCTATTC *inter56* R1: ATAGCCCCCAACCTACAAGC *inter56* R1B: GGACAAGATGCGGCTCTATTC	Wt: 796bp Mutant: 363bp

Table 2.Primers in 5' to 3' orientation used to screen for *dlx* mutant lines as well as their expected band sizes

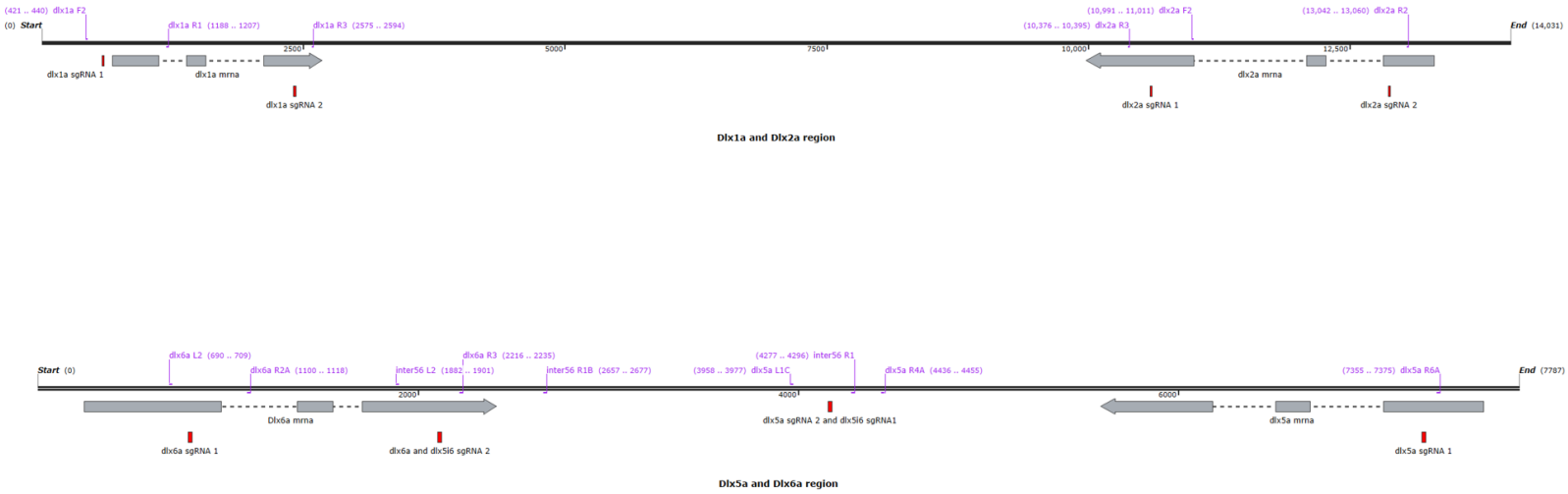

Figure 5. Zebrafish *dlx1/2* and *dlx5/6* bigenes labeled with sgRNA and primer binding sites. Zoom in for additional clarity.

2.2 Histology and cryosectioning

Adult zebrafish were euthanized by immersion in an ice-water bath for 10 minutes, followed by decapitation. Heads were subsequently fixed in 4% paraformaldehyde (PFA) at 4 °C for 24 hours. Following fixation, whole brains were carefully dissected and washed three times for 5 minutes each in phosphate-buffered saline (PBS). Tissues were then cryoprotected by immersion in a 30% sucrose solution at 4 °C for an additional 24 hours.

After cryoprotection, whole brains were embedded in tissue tek optimal cutting temperature (OCT) compound (4583) within disposable base molds, 7 x 7 x 5mm (27147-1) , rapidly frozen using liquid nitrogen, and stored at −20 °C until further processing. Cryosectioning was performed using a Leica CM1850 cryostat to obtain sections ranging from 16 to 18 µm in thickness. Sections were mounted onto glass slides (MSL3X1) and stored at −20 °C prior to staining.

2.3 Immunohistochemistry

Tissue sections first underwent antigen retrieval to unmask our target proteins by incubation in 0.01 M sodium citrate buffer containing 0.05% Tween-20 at 85 °C for 20 minutes. Slides were then allowed to cool at room temperature for 15 minutes and washed twice for 5 minutes in 1× phosphate-buffered saline (PBS). Sections were subsequently washed in PBS-DT (1xPBS, 1% BSA, 1% DMSO, 1% triton x) for 2 × 15 minutes at room temperature, followed by blocking in 300–500 µL of blocking solution (20% fetal bovine serum in PBS-DT) for 2 hours at room temperature. Slides were then incubated overnight at 4 °C with primary antibody diluted in antibody solution (5% fetal bovine serum with antibodies in PBSTx) under coverslips.

The following day, sections were washed in PBS-DT (6 × 15 minutes) to remove excess primary antibody, and then incubated overnight at 4 °C with the appropriate secondary antibody (Table 3) diluted in antibody solution. On the third day, slides were washed again in PBS-DT (6 × 15 minutes), followed by a 5-minute wash in PBS and a brief rinse in distilled water. Sections were then air-dried completely before mounting with VECTASHIELD mounting medium containing DAPI (H-1200-10). Coverslips were applied, sealed with nail polish, and slides were stored at 4 °C until imaging.

Host Organism	Target	Supplier Information	Dilution
Mouse	Calretinin	Swant, 6B3	1:400
Mouse	Parvalbumin	Swant, PV 235	1:400
Goat	Mouse IgG (H+L)	Thermo Fischer Scientific	1:1000

Table 3. Antibodies used in immunohistochemistry experiments

2.4 Fluorescent In situ Hybridization

Unfortunately, Immunohistochemistry on SST is not possible in zebrafish meaning we have to use FISH instead. For in situ hybridization, slides were first thawed at room temperature for 15 minutes. Sections were permeabilized by incubation in 0.3% Triton X-100 in DEPC-treated PBS (pH 7.4) for 15 minutes, followed by two 5-minute washes in DEPC-PBS. To enhance probe accessibility, sections were treated with Proteinase K (5 µg/mL) for 15 minutes, then washed twice for 5 minutes in DEPC-PBS. Tissue was subsequently refixed in 4% paraformaldehyde (PFA) in PBS for 20 minutes to stabilize morphology and improve tissue adherence, followed by two additional 5-minute washes in DEPC-PBS.

Sections were then acetylated for 5 minutes in a freshly prepared solution containing triethanolamine and acetic anhydride in DEPC-treated water to reduce non-specific probe

binding. Slides were washed twice for 5 minutes in DEPC-treated water and allowed to air dry. For hybridization, our probe was diluted in hybridization buffer (1× salt, 50% deionized formamide, 10% dextran sulfate, yeast tRNA at 1 mg/mL, and 1× Denhardt's solution, in d.d.H_2O) (1:1000), vortexed, and denatured at 70 °C for 5–10 minutes. A volume of 500 µL of probe mixture was applied to each slide, which was then coverslipped and incubated overnight at 70 °C in a sealed chamber.

Following hybridization, coverslips were removed and sections were subjected to post-hybridization washes consisting of two 30-minute washes at 70 °C in solution A (1XSSC, 50% formamide,0.1% tween 20 in d.d.H20), followed by two 30-minute washes at room temperature in TBST (1.4 M NaCl, 27 mM KCl, 0.25 M Tris HCl, 1% Tween 20 or Triton X, in d.dH2O at pH 7.5). Endogenous peroxidase activity was quenched by incubation in 2% hydrogen peroxide in TNT buffer for 10 minutes, followed by four 5-minute washes in TNT (0.1 M Tris-HCl pH 7.5, 0.15 M NaCl, 0.5% Tween-20). Sections were then blocked by incubation in TBSTB for 2–4 hours in a humidified chamber.

After blocking, slides were washed sequentially in TNT (2 × 5 minutes, 2 × 10 minutes, followed by 20- and 30-minute washes). Signal amplification was performed by incubating sections for 10 minutes in amplification diluent containing 1:100 tyramide–fluorescein, followed by a 5-minute wash in TNT and two additional 5-minute washes after coverslip removal. Finally, slides were briefly rinsed in water to remove residual salts and mounted using VECTASHIELD mounting medium containing DAPI.

Target	Forward Primer	Reverse Primer
SST	SST-1 F1: ATAAAAGATGCTCTCCACGCG	SST-1 R1 +T7: TAATACGACTCACTATAGGACACATCAATATAGCCTCGG

Table 4. Primers used for SST probe generation

2.5 Image analysis and Cell Counting

Fluorescent images of immunohistochemistry and in situ hybridization samples were acquired using an Olympus FV1000 BX61 laser scanning confocal microscope. Z-stack images were collected to capture signal throughout the full depth of the tissue. Quantification was performed by manual cell counting using FIJI 2.18.0 a modified version of the software image J. For each genotype an average of 3 brains were imaged with multiple sections from each. All positive cells in our ROI were counted and used for statistical analysis. All cell counting were conducted blind to sample genotype to minimize bias.

2.6 CDNA preparation and qPCR

Total RNA was isolated from whole zebrafish 24hpf embryos using TRIzol (Thermo Fischer 15596026) Approximately 100 larvae were homogenized in 1 mL of TRIzol, ensuring that the sample volume did not exceed 10% of the reagent volume. Samples were mechanically homogenized using pipette tips, vortexed, and re-homogenized to ensure complete disruption, then incubated for 5 minutes at room temperature to allow dissociation of nucleoprotein complexes. Chloroform (0.2 mL per 1 mL TRIzol) was subsequently added, and samples were vigorously vortexed for 15 seconds, incubated for 2–3 minutes at room temperature, and centrifuged at 12,500 RPM for 10 minutes to achieve phase separation.

The aqueous phase was carefully transferred to a new tube, and RNA was precipitated by adding 0.5 mL isopropanol per 1 mL TRIzol, followed by a 10-minute incubation at room temperature and centrifugation at 12,500 RPM at 4 °C for 15–20 minutes. The resulting RNA pellet was washed once with 75% ethanol, briefly vortexed, and centrifuged at 10,000 RPM for 5 minutes. Finally, the pellet was air-dried and resuspended in 20 µL of RNase-free water, incubated at 55–60 °C for 10 minutes to facilitate dissolution, and stored at −80 °C until further use.

Isolated RNA was subsequently reverse-transcribed into complementary DNA (cDNA) using the iScript cDNA Synthesis Kit (Bio-Rad), according to the manufacturer's instructions. The resulting cDNA was then used in downstream applications, including qPCR primer optimization and quantitative PCR (qPCR) analysis.

2.7 Bioinformatics

Publicly available transcriptomic datasets (Farrell et al., 2018; Sur et al., 2023) were analyzed using the Danio Cell platform to investigate gene expression patterns in zebrafish. Gene expression profiles for *dlx* family members were queried across developmental stages and cell populations using the platform's integrated visualization and analysis tools. Data generated from Danio Cell (https://daniocell.nichd.nih.gov/) were used to contextualize ideas about dlx gene expression patterns in relation to their complex organization and serve as a sort of proof of concept for potential qPCR experiments.

2.8 Statistical Analysis

Statistical analyses were conducted using Microsoft Excel (Office home and student 2019) and BioRender's statistical tools. Parvalbumin (PV), somatostatin (SST), and calretinin (CR) neuron counts across the different *dlx* mutant lines were compared using a two-tailed Student's *t*-test assuming unequal variances. A p value ≤ 0.05 was chosen to mark significance. Error bars represent the standard error of the mean (SEM), and sample sizes for each experiment are indicated in the corresponding figure legends.

3. Results

3.1 Impact of *dix* mutations on populations of zebrafish GABAergic interneurons

The objective of this chapter is to employ two histological techniques, immunohistochemistry and fluorescence in situ hybridization, to characterize and quantify the impact of *dlx* gene deletions on GABAergic neuron development in zebrafish. By examining multiple proteins (Parvalbumin and Calretinin) and mRNA (Somatostatin) this work aims to define the specific contributions of individual *dlx* paralogs to the development, of GABAergic neurons within the zebrafish central nervous system.

3.1.2 dlx1a and dlx5a are essential in somatostatin interneuron development.

The purpose of this section is to employ FISH to quantify the impact of *dlx* gene deletions on SST+ neuronal populations within the anterior and posterior parvocellular preoptic area of the zebrafish brain. By examining changes in SST+ neuron abundance across the mutant lines, this work aims to further elucidate the role of individual *dlx* paralogs in the development and maintenance of distinct GABAergic interneuron subpopulations within the preoptic region.

Quantification of SST^+ neurons across the examined *dlx* mutant zebrafish lines reveals a gene-specific impact on this interneuron population, with both reductions and relative preservation depending on the genotype. In *dlx1a* $^{(-/-)}$ and *dlx5a* $^{(-/-)}$ mutants, a statistically significant decrease in SST^+ neuron number is observed compared to WT siblings, indicating that these genes play an important role in the development or maintenance of SST-expressing

neuronal populations (Figures 5 and 6). A similar downward trend is present in *dlx2a* $^{(-/-)}$ mutants; however, this reduction does not reach statistical significance due to small sample size of *dlx2a* $^{(-/-)}$ mutants. In contrast, *dlx6a* mutants do not exhibit a reduction in SST^{+} neurons and instead show a slight, non-significant increase relative to WT, implying that *dlx6a* $^{(-/-)}$ may not be critically required for SST interneuron specification, or that compensatory mechanisms may offset its loss. The *inter56* mutant similarly does not display a statistically significant difference, although a modest decrease is observed. This is not necessarily too abnormal as this line is simply a KO of the intergenic enhancers and there effects might be more modest when compared to a gene KO line.

These findings are consistent with previous studies in mice demonstrating that the *Dlx1/2* bigene cluster is essential for proper development of somatostatin-positive (SST+) interneurons(Cobos et al., 2005b; Pla et al., 2018). However, prior research has largely focused on the role of the *Dlx1/2* cluster, with comparatively little attention given to the contribution of the *Dlx5/6* bigene. The results obtained in this study expand upon this existing body of work by demonstrating that *dlx5a* is also critically involved in SST+ neuron development in zebrafish. This suggests that regulation of SST interneuron specification may involve a broader and more interconnected *dlx* regulatory network than previously appreciated, with both bigene clusters contributing to the establishment and maintenance of this GABAergic neuronal subtype.

In conclusion, the results of this study indicate that both *dlx1a* and *dlx5a* play important roles in the development of SST+ neurons within the PPa and PPp of the zebrafish brain. The data further suggest that *dlx2a* may also contribute to the development of these neuronal populations; however, additional biological replicates and increased sample sizes will be

required before definitive conclusions can be drawn regarding its specific role. Importantly, the variability observed within wild-type control groups, as well as the relatively large error bars present in certain experimental conditions, indicate the presence of technical variation that may influence the robustness of the observed phenotypes. These limitations emphasize the need for further replication in future studies.

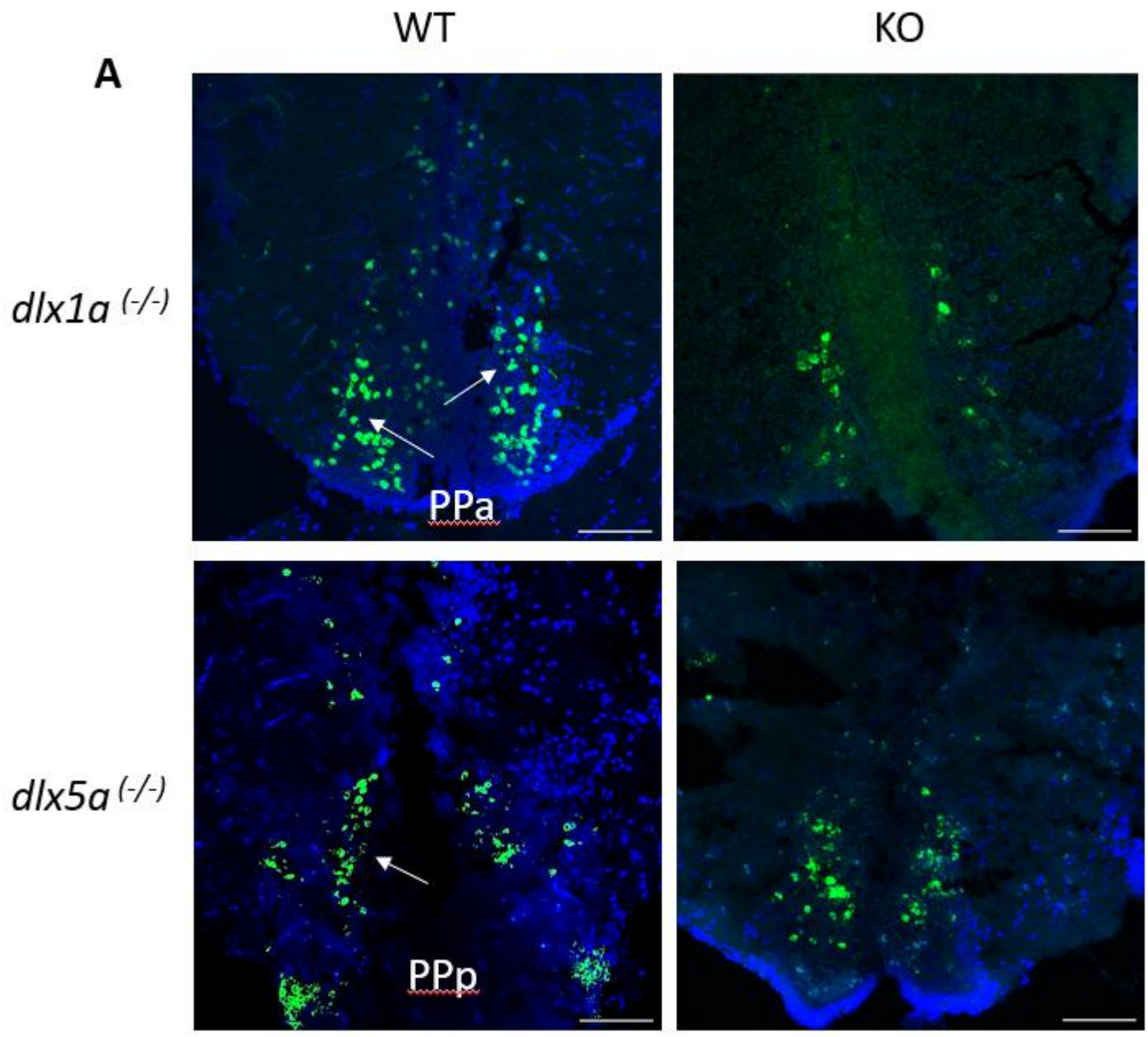

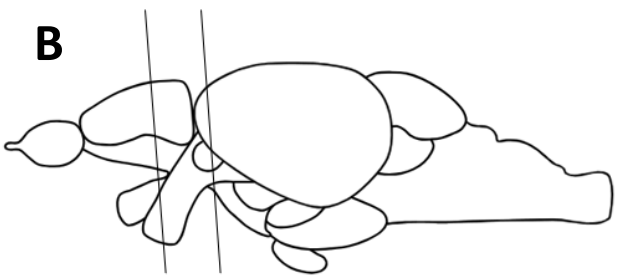

Figure 6. Representative images of SST FISH in *dlx* mutant zebrafish. (A) Representative images comparing SST expression detected by FISH in the anterior PPa and PPp of *dlx1a* and *dlx5a* mutant zebrafish and their respective WT controls. Scale bars correspond to 100µm. (B) Schematic representation of the zebrafish brain indicating the anatomical locations of the PPa and PPp regions analyzed.

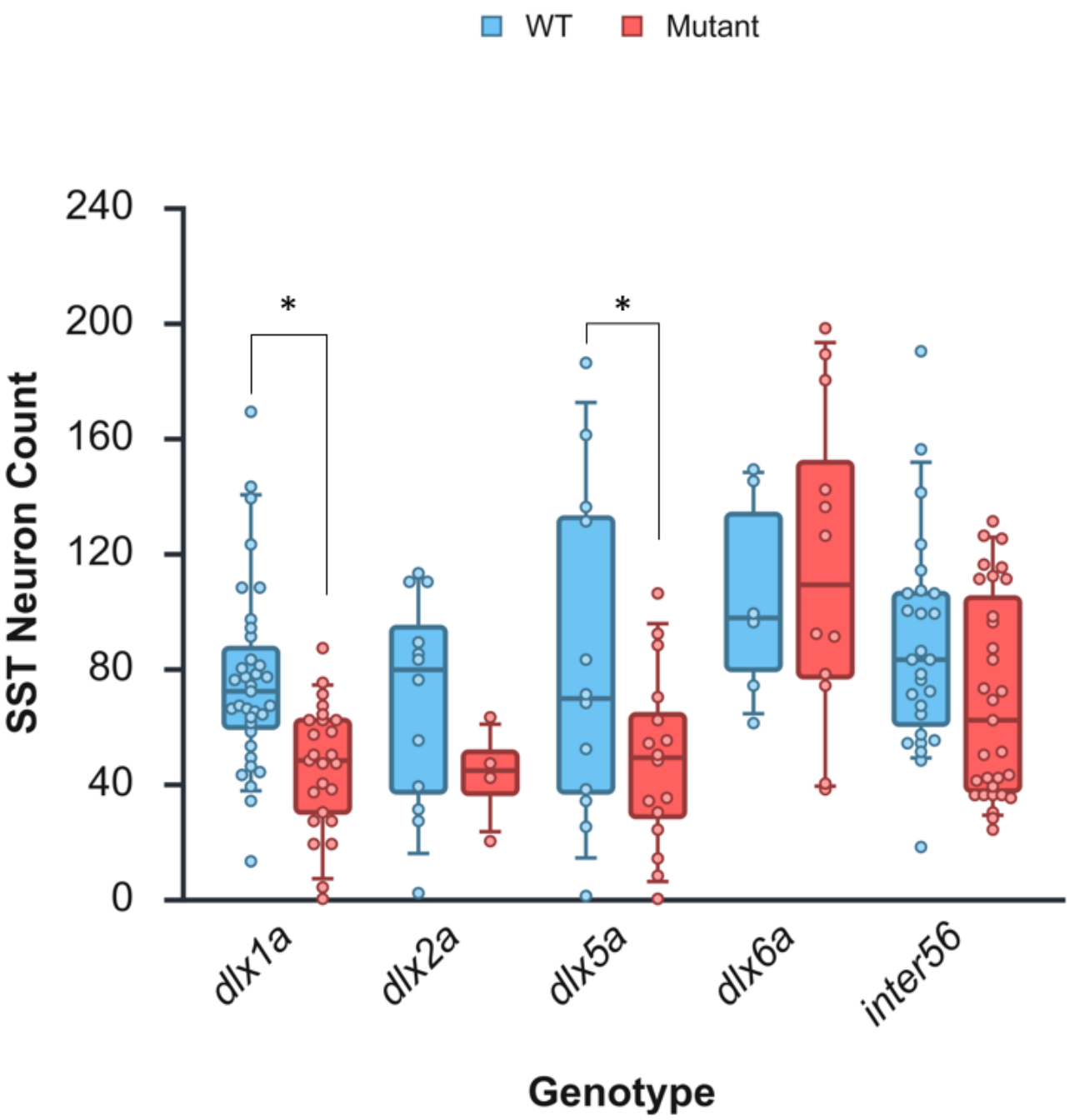

Figure 7. Quantification of SST interneurons in the PPa and PPp across zebrafish genotypes.
Bar graph illustrating the mean ± SEM number of SST interneurons identified by FISH in WT (Blue) and Mutant (Red) zebrafish for each genotype examined. An average of 15 sections from 3 brains were analyzed for each genotype. A reduction in SST^{+} interneuron number is observed in KO animals relative to their WT counterparts for the indicated genotypes. Statistical analyses were performed using a two-tailed Student's *t*-test assuming unequal variances (heteroscedastic). Statistical significance is denoted by asterisks ($p < 0.05$).

3.1.3 *dlx2a* and *dlx5a* are essential in Calretinin interneuron development.

The objective of this chapter is to quantify the impact of *dlx* gene deletions on CR+ interneuron populations within TeO of the zebrafish brain using IHC. By comparing CR+ neuron abundance across the various mutant lines, this work aims to further characterize the role of individual *dlx* paralogs in the development and maintenance of distinct GABAergic interneuron subtypes within the zebrafish central nervous system.

The quantification of CR^+ interneurons revealed a significant reduction in cell number in both dlx mutant lines compared to wildtype controls (Figure 7 and 8). In $dlx2a^{-/-}$ mutant fish, CR^+ cell counts were markedly decreased, with median values around ~150 cells compared to ~380–400 cells in wildtype. This difference was highly significant, indicating a strong requirement for *dlx2a* in the proper development or development of CR-expressing interneurons in the TeO. A similar trend was observed in $dlx5a^{-/-}$ mutants, where median CR^+ cell counts (~170 cells) were substantially lower than those of wildtype siblings (~390–420 cells), again reaching high statistical significance. In both cases, although some variability was present within groups, the distributions of mutant and wildtype populations showed limited overlap, with wildtype consistently exhibiting higher CR^+ neuron counts. Notably, the comparable magnitude of reduction between *dlx2a* and *dlx5a* mutants suggests that these genes may play overlapping or cooperative roles in regulating CR^+ interneuron development. Together, these findings demonstrate that loss of dlx gene function leads to a pronounced depletion of CR-expressing neuronal populations, supporting a critical role for dlx genes in the specification of this interneuron subtype.

Further analysis of the other *dlx* mutant fish was unable to be performed despite having stained every genotype due to a strange occurrence of staining fading. The same exact sample imaged a few weeks apart revealed a marked decrease in the number of positively stained CR neurons meaning any sort of comparison done on these slides would be inaccurate at best. However, with as effective as the staining is in the future this problem can be simply resolved by imaging the samples shortly after their initial staining.

In conclusion, the findings presented in this chapter demonstrate that both *dlx2a* and *dlx5a* are important for the proper development of CR+ neurons within the TeO of the zebrafish brain. The observed reductions in CR+ neuronal populations within these mutant lines suggest that these paralogs play significant roles in the specification of this interneuron subtype. However, further analysis of the remaining *dlx* mutant lines will be necessary to fully elucidate the individual and potentially overlapping contributions of each *dlx* paralog to CR+ neuron development and to better understand the broader regulatory network governing GABAergic interneuron differentiation.

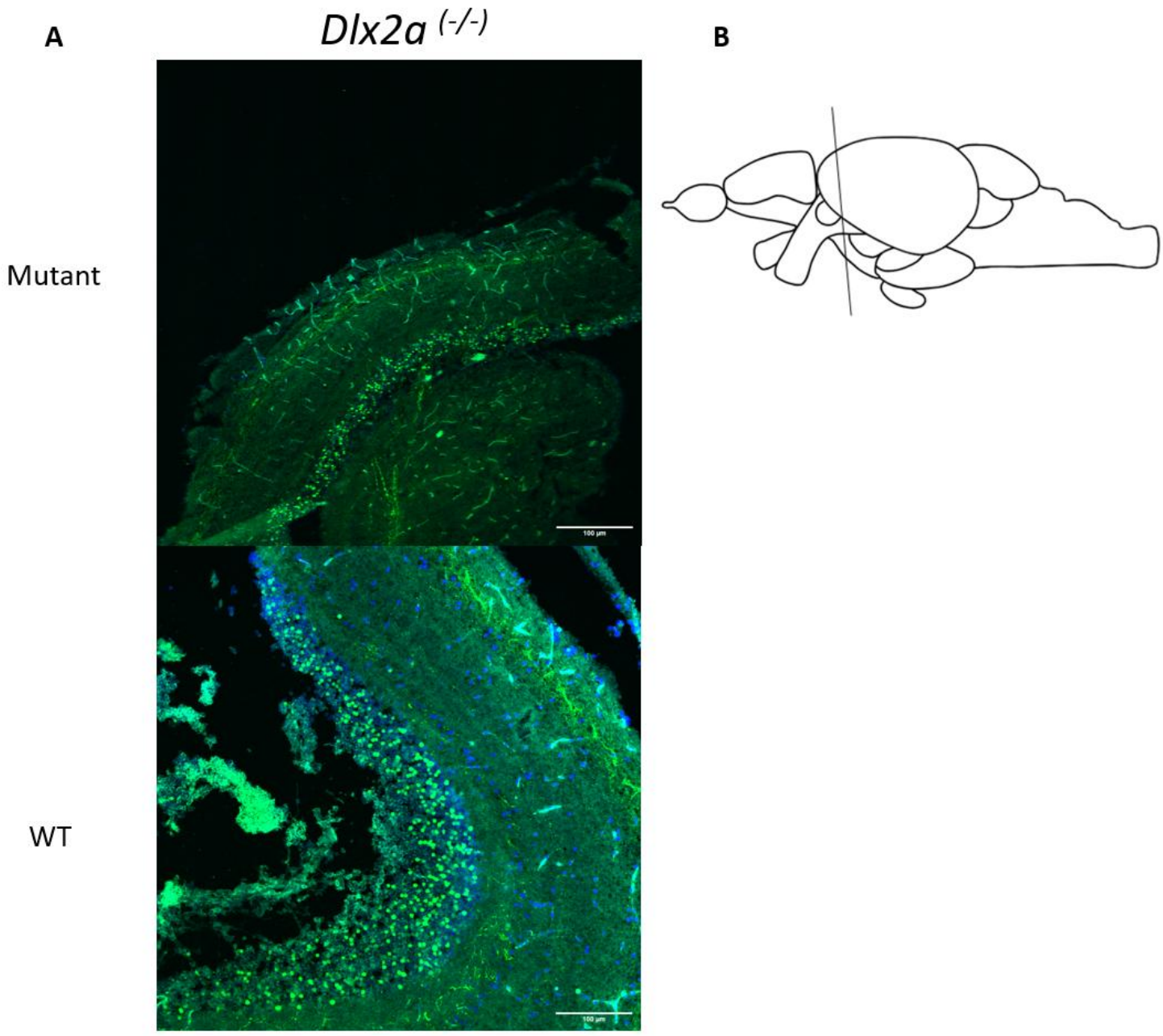

Figure 8. Representative images of CR immunostaining in *dlx2a* mutant zebrafish.
(A) Representative images of CR-immunostained sections from the TeO of *dlx2a* mutant zebrafish and their WT siblings, enabling comparison of CR-positive cell distribution between genotypes. B) Schematic representation of the zebrafish brain indicating the anatomical location of the TeO.

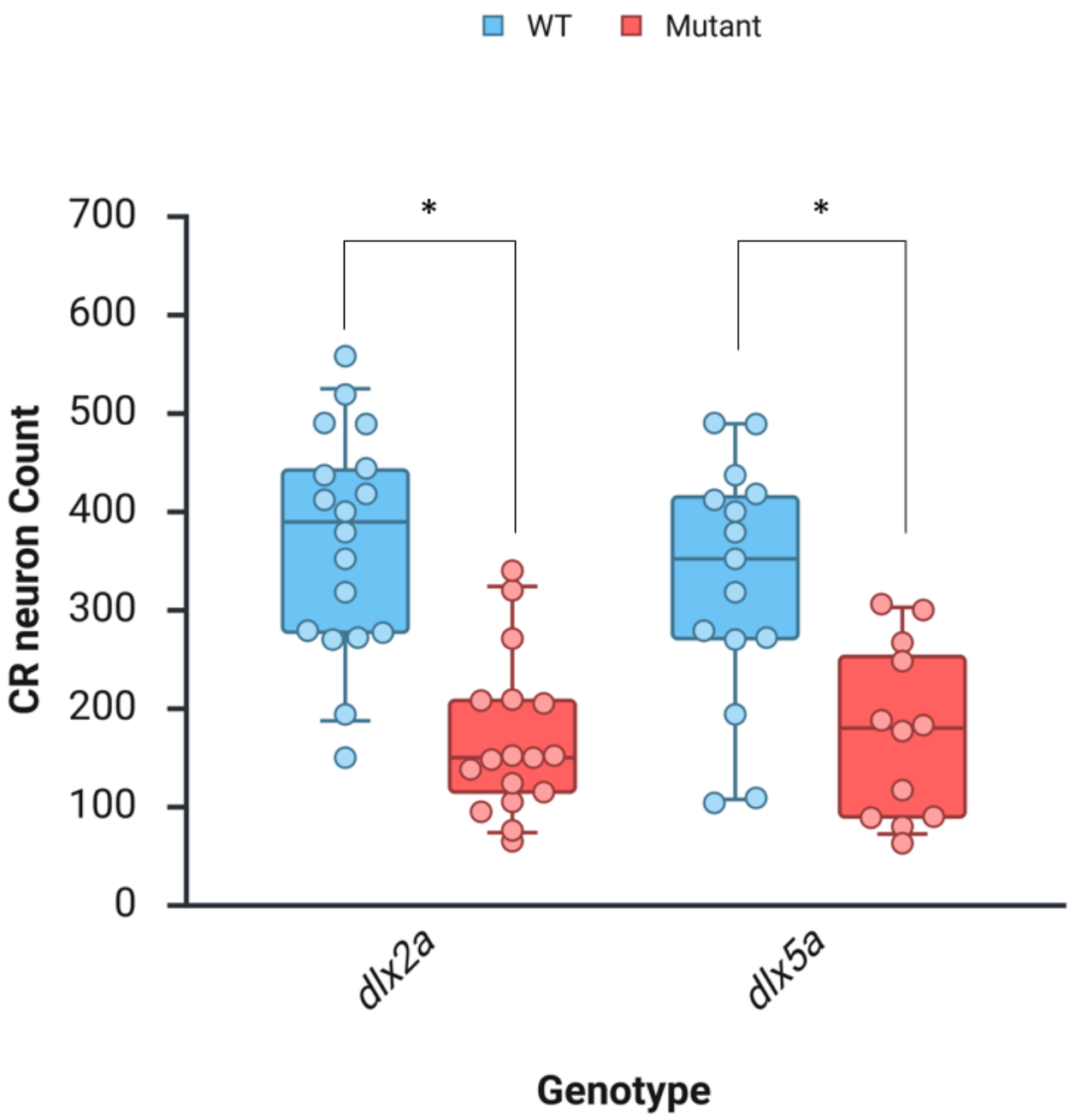

Figure 9. Quantification of CR interneurons in mutant zebrafish TeO. Bar graph illustrating the mean ± SEM number of CR^+ interneurons identified by immunohistochemistry in WT (Blue) and Mutant (Red) zebrafish. An average of 15 sections from 3 brains per genotype were analysed. A reduction in CR^+ interneuron number is observed in KO animals relative to their WT counterparts for both genotypes. Statistical analyses were performed using a two-tailed Student's *t*-test assuming unequal variances (heteroscedastic). Statistical significance is denoted by asterisks ($p < 0.05$).

3.1.4 *dlx* gene family overall important for parvalbumin interneuron development.

The objective of this section is to quantify parvalbumin-positive (PV+) GABAergic interneurons within the optic tectum of the zebrafish brain across our mutant lines. By examining changes in this specific interneuron population, this work aims to more precisely define the individual contributions of each *dlx* paralog to GABAergic neuron development and maturation.

Quantitative analysis of PV+ interneurons across multiple *dlx* mutant zebrafish lines revealed a clear and gene-specific impact on PV+ neuron populations in the TeO. In almost all genotypes examined WT animals consistently exhibited higher numbers of PV^+ interneurons compared to their knockout KO counterparts; however, the magnitude and statistical significance of this reduction varied between lines. Significant decreases in PV+ cell number were observed in *dlx1a*$^{(-/-)}$, *dlx5a*$^{(-/-)}$, *dlx5i6*$^{(-/-)}$, and *dlx6a*$^{(-/-)}$ mutants, supporting a role for these genes in the development, PV-expressing interneurons. Among these, *dlx5a*$^{(-/-)}$ mutants displayed the most pronounced reduction, suggesting that *dlx5a*$^{(-/-)}$ may play a particularly prominent or non-redundant role in regulating PV interneuron specification. Similarly, the combined *dlx5i6*$^{(-/-)}$ mutant exhibited a strong decrease in PV^+ cells, consistent with the known functional redundancy and cooperative activity of these paralogous genes in forebrain development. In contrast, the *dlx2a*$^{(-/-)}$ mutant did not show a statistically significant difference relative to WT siblings, indicating that *dlx2a*$^{(-/-)}$ alone may be dispensable for PV interneuron development, or that its function is compensated for by other *dlx* family members in this context.

However, it is important to note that, despite optimization of the staining protocol and visualization of PV^+ interneurons (Figures 9 and 10), the overall cell counts remained low across all conditions. This is rather surprising considering our understanding of PV+ neurons in the brain. Previous work on mice has established that GABAergic interneurons represent 40% of cortical interneurons (Druga et al., 2023) Similar quantification in the zebrafish has not been extensively performed so it is unclear whether PV+ neurons represents such a major population in our model, however previous research staining for PV+ neurons in zebrafish larvae found around 80+ PV+ neurons on average throughout several brain regions including the TeO, a much larger number than we found with our staining (D'Gama et al., 2024). Furthermore, the number of PV^+ cells quantified in WT controls displayed notable variability between samples, whereas consistent values would be expected. This variability must be addressed before satisfying conclusions could be made as to the impact of the *dlx* genes on PV^+ neuron development.

In conclusion, a net reduction in PV+ neurons was observed within the TeO of zebrafish across all mutant lines examined, with the exception of the *dlx2a* $^{(-/-)}$ line. However, interpretation of these findings should be approached cautiously due to the variability observed between control groups and the low levels of PV staining obtained compared to previously published studies. These limitations suggest the need for further methodological refinement and experimental validation before definitive conclusions regarding the impact of *dlx* deletions on PV+ interneuron populations can be drawn.

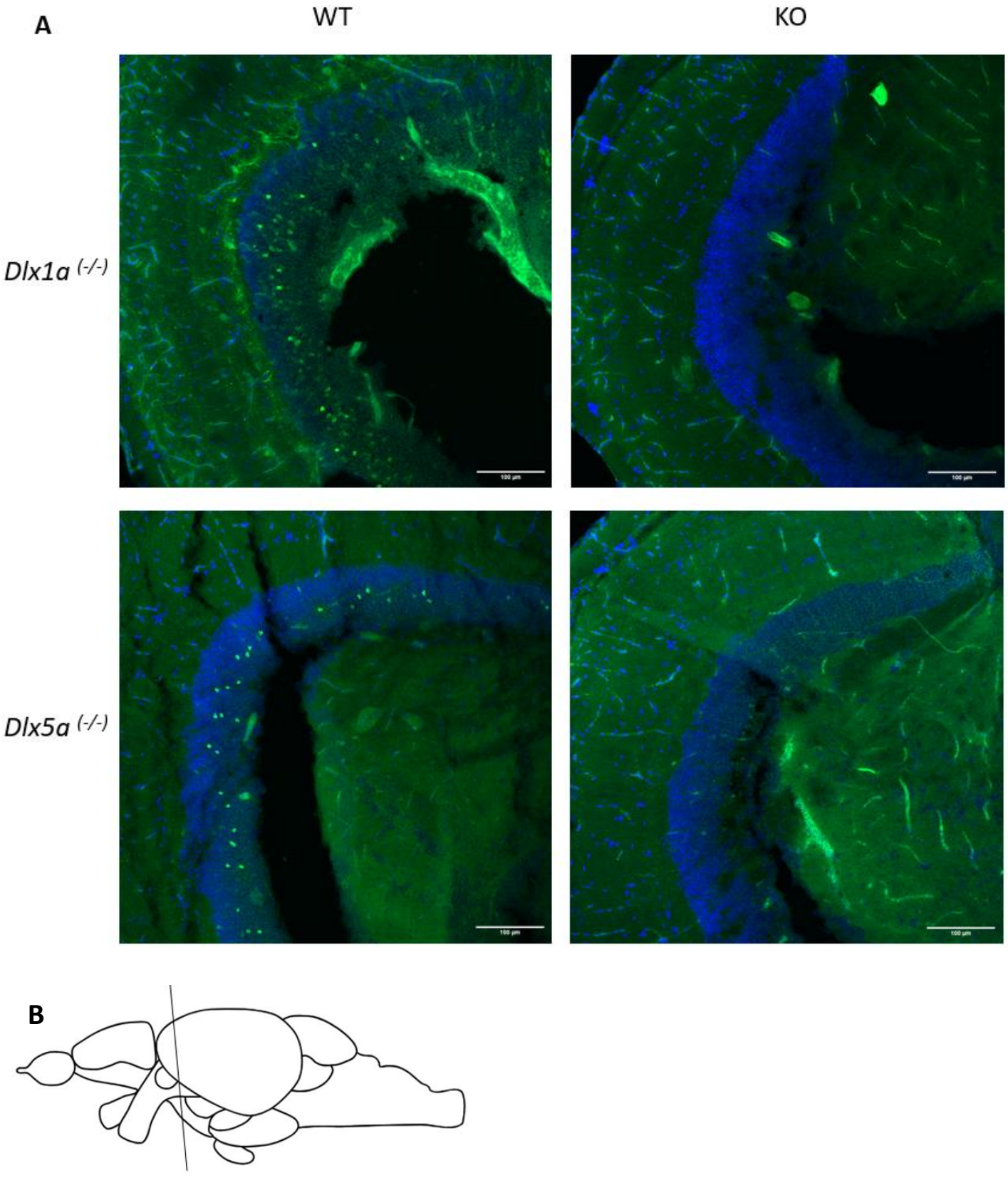
A
WT
KO
Dlx1a (-/-)
Dlx5a (-/-)
B

Figure 10. Representative images of PV immunostaining in wild-type and dlx1a mutant zebrafish.
(A) Representative images of PV-stained PGZ tissue from a *dlx1a* and *dlx5a* wild-type fish and mutant siblings, demonstrating a marked reduction in PV-positive cells in the mutants.
(B) Schematic illustration of the zebrafish brain indicating the anatomical location of the sections analyzed.

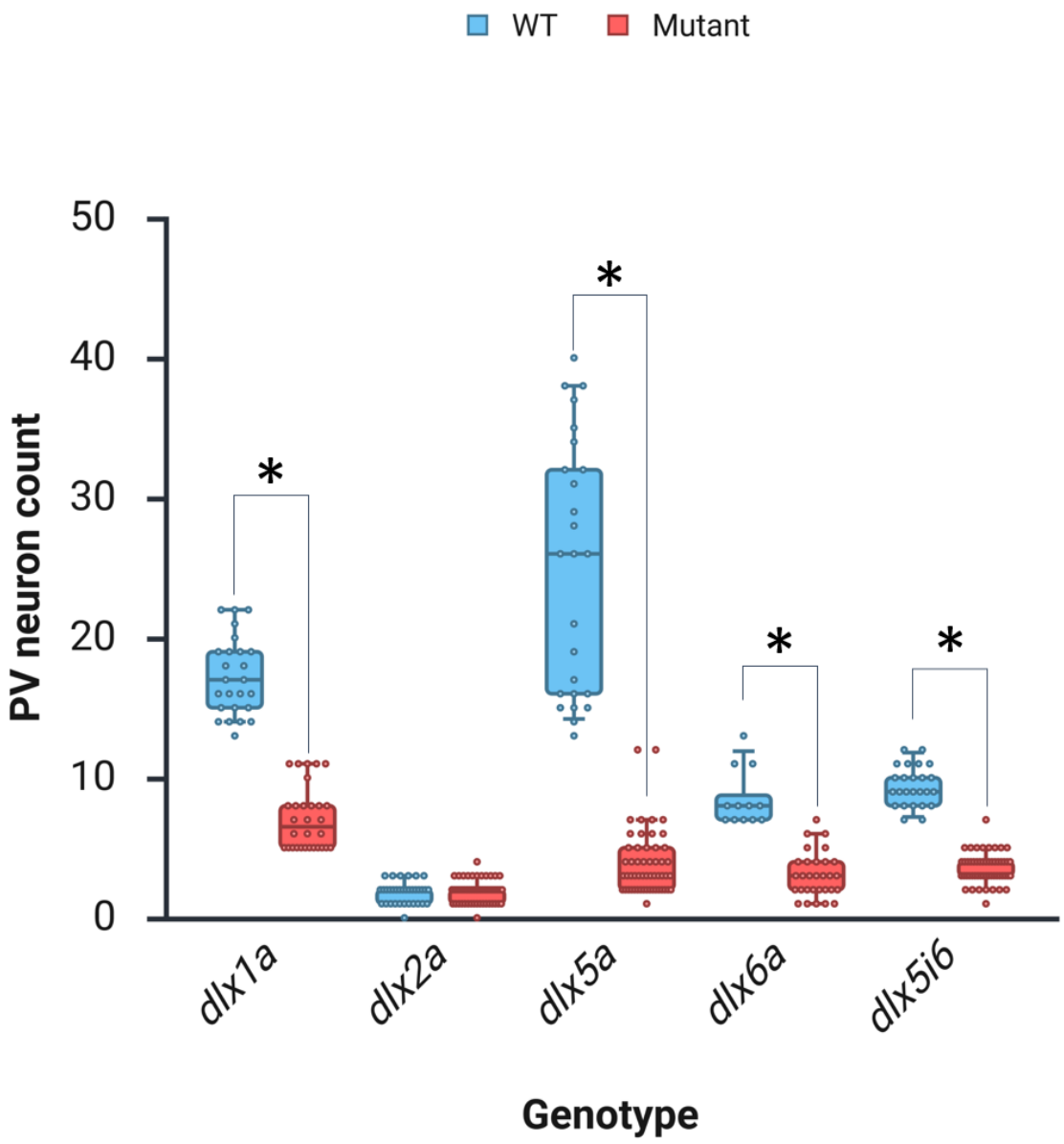

Figure 11. Quantification of PV-positive interneurons in the TeO across zebrafish genotypes.
Bar graph illustrating the mean ± SEM number of PV^+ interneurons identified by immunohistochemistry in WT (Blue) and KO (Red) zebrafish for each genotype examined. An average of 25 sections per genotype were analysed from 3 different brains. A reduction in PV^+ interneuron number is observed in KO animals relative to their WT counterparts for the indicated genotypes. Statistical analyses were performed using a two-tailed Student's *t*-test assuming unequal variances (heteroscedastic). Statistical significance is denoted by asterisks ($p < 0.05$), while "ns" indicates non-significant differences ($p > 0.05$)

3.2 Optimizing *dlx* mRNA quantification via qPCR.

The objective of this section of the thesis is to develop and optimize a reliable qPCR-based approach for quantifying *dlx* transcript levels. Achieving this goal proved more challenging than initially anticipated, largely due to inherent features of the *dlx* gene family, including their low expression levels and compact genomic architecture. These characteristics complicate primer design and increase susceptibility to technical issues such as nonspecific amplification and genomic DNA contamination, necessitating extensive optimization to establish a reproducible protocol.

3.2.1 Troubleshooting *dlx* quantification via qPCR

Standard qPCR primer design strategies typically reduce gDNA contamination by positioning forward and reverse primers on separate exons flanking one or more intronic regions. Under these conditions, amplification from contaminating gDNA is minimized because the larger intron-containing template is less efficiently amplified during the short extension times used in qPCR. However, despite designing primers according to these conventional guidelines, in our initial qPCR experiments NRT controls displayed substantial amplification indicative of gDNA contamination (Figure 11). This likely is due to the compact genomic architecture of the *dlx* gene family, which is characterized by short coding regions and small introns. Consequently, even primers spanning one or more introns were still capable of efficiently amplifying residual gDNA present in the samples, resulting in unreliable expression data. These findings demonstrated that additional optimization of RNA purification and primer design was required before accurate qPCR analyses could be performed.

The initial strategy to address gDNA contamination focused on reducing its presence prior to qPCR through a series of RNA treatment approaches (Figure 12). In untreated samples, substantial gDNA contamination was evident, as indicated by the presence of multiple bands on diagnostic gels, with higher molecular weight bands corresponding to intron-containing gDNA amplicons. This pattern was observed across most targets, with the exception of the housekeeping gene *rpl13a* and *dlx2a*, which showed comparatively minimal contamination. Pre-treatment of RNA samples with DNase I prior to cDNA synthesis significantly reduced gDNA contamination to undetectable levels for most genes, although low-level contamination persisted for *dlx6a*. Similarly, purification using a RNeasy RNA cleanup kit effectively eliminated detectable gDNA in all but *dlx1a*. Notably, combining DNase I treatment with RNeasy purification resulted in no visible gDNA contamination across all targets.

qRT-PCR analysis revealed a limitation of these approaches. Specifically, all treatment conditions resulted in a substantial reduction in total RNA yield and concentration. Consequently, qPCR amplification occurred at very late cycle thresholds ($Ct \geq 35$), approaching the limits of reliable detection and raising concerns regarding data validity based on established qPCR standards. Furthermore, the increased sensitivity of qPCR relative to endpoint PCR meant that even trace levels of residual gDNA contamination could still be detected, compounding the ambiguity of the results. This issue is worsened by the *dlx* genes, which are transcription factors expressed at low endogenous levels; thus, any reduction in RNA input disproportionately impacted their representation in the resulting cDNA pool. Collectively, these findings demonstrated that while pre-treatment strategies could reduce detectable gDNA contamination, they simultaneously compromised RNA integrity and yield to a degree that

precluded reliable qPCR analysis. Therefore, an alternative approach was required to achieve accurate and reproducible quantification of *dlx* gene expression.

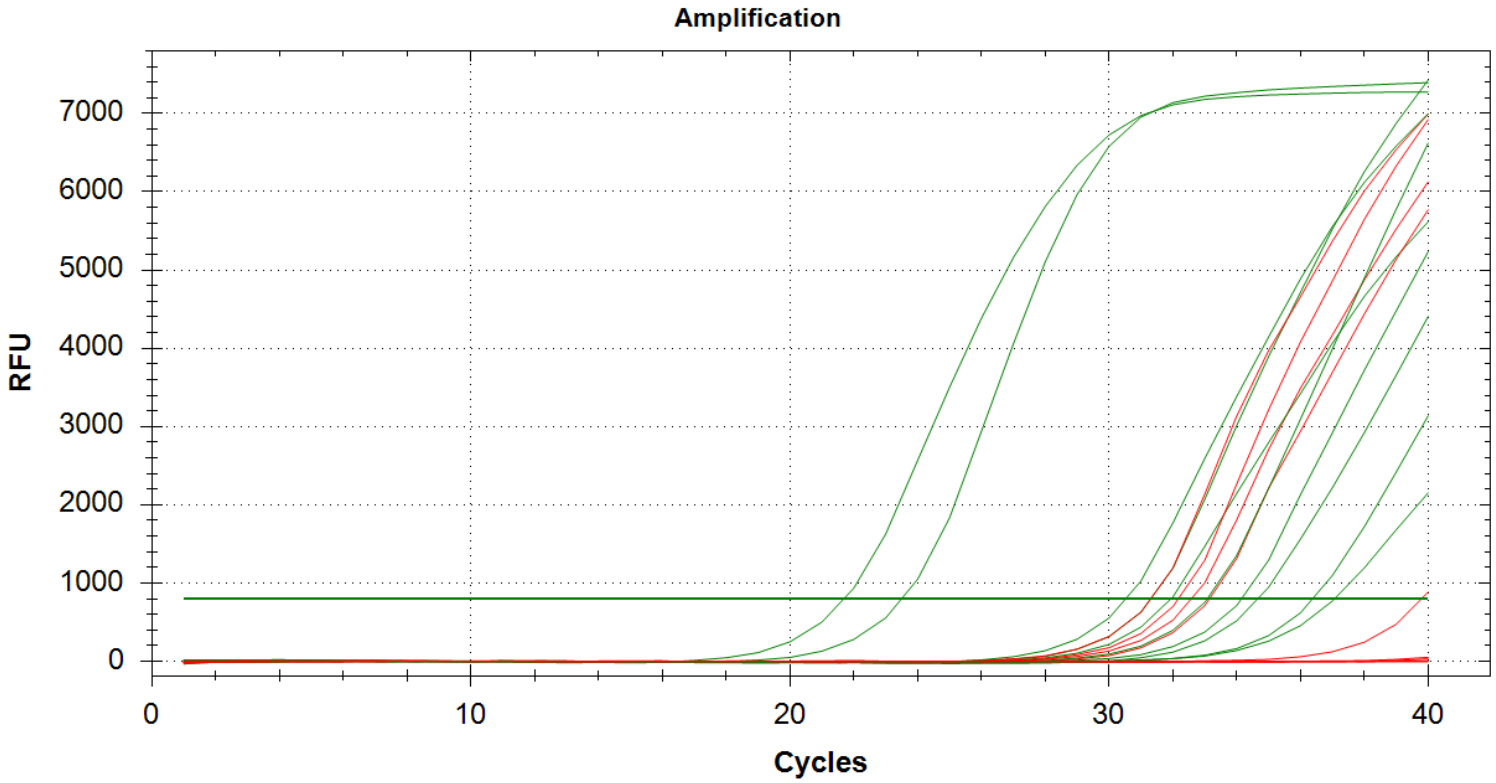
Amplification
RFU
7000
6000
5000
4000
3000
2000
1000
0
0
10
20
30
40
Cycles

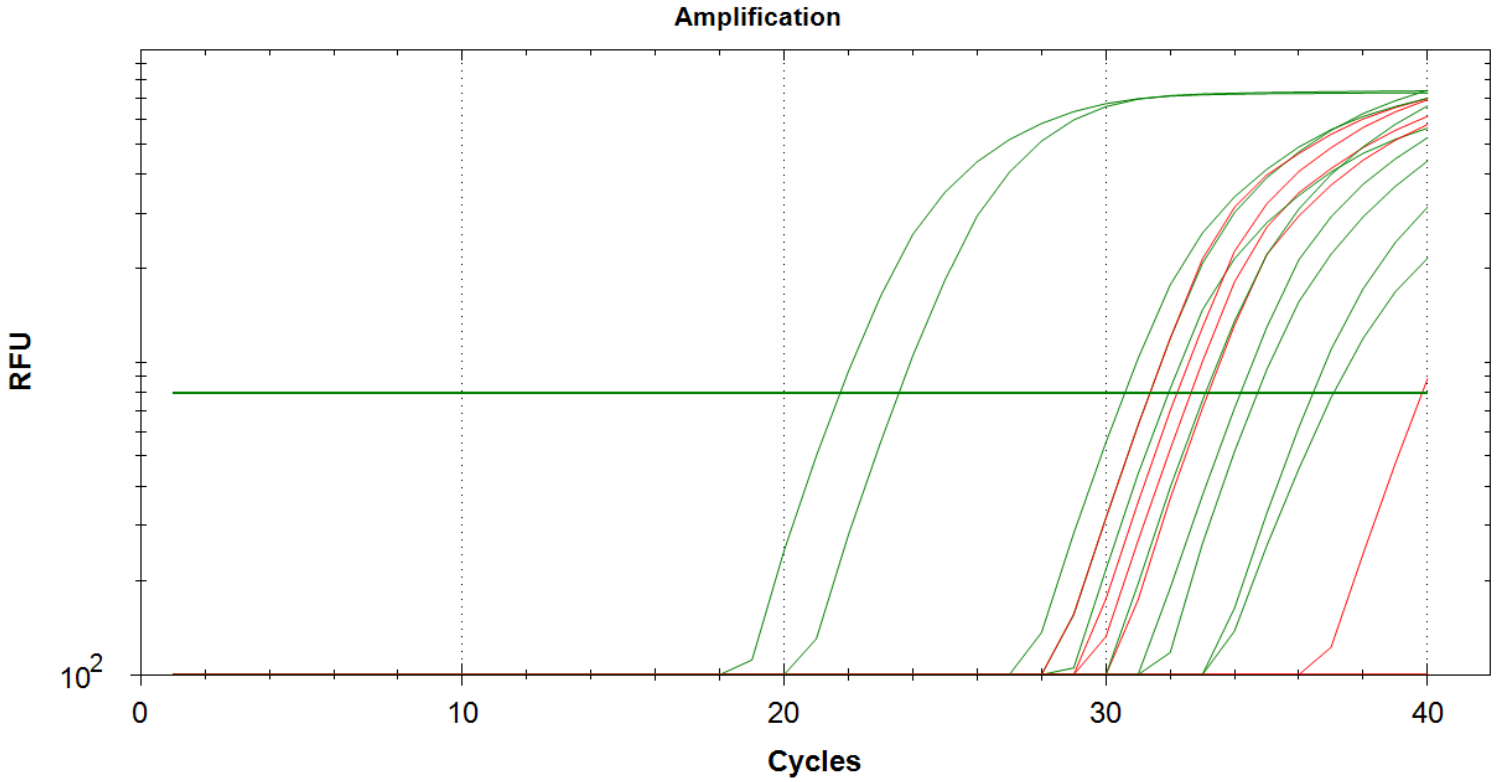
Amplification
RFU
10^2
0
10
20
30
40
Cycles

Figure 12. *dlx* qPCR trial run. Primer sets targeting four *dlx* genes (*dlx1a*, *dlx2a*, *dlx5a*, and *dlx6a*) were assessed alongside the housekeeping gene *rpl13a*. Amplification curves for experimental samples are shown in green, while negative controls (NRT and no template control NTC) are shown in red. In this initial trial, *dlx* targets amplify relatively late (≈30 cycles), and substantial signal is observed in control reactions indicating contamination. These results highlight the need for further optimization of the qPCR assay.

Figure 13. Diagnostic gel assessing genomic DNA removal following RNA purification and cDNA synthesis. Agarose gel electrophoresis of PCR products generated using standard PCR conditions matching the annealing temperatures and cycling parameters used for subsequent qPCR analyses. Templates consisted of cDNA synthesized using the Bio-Rad iScript reverse transcription kit from RNA isolated by TRIzol extraction. Treatments from left to right were: untreated control, DNase I treatment, RNeasy purification kit treatment, and combined DNase I plus RNeasy purification treatment. This analysis was performed to evaluate the relative effectiveness of each method in reducing genomic DNA contamination prior to downstream qPCR applications.

To overcome this contamination issue, a new generation of primers were designed. Unlike the original primer sets, which were positioned on separate exons, the revised design incorporated a reverse primer spanning an exon–exon junction (Figure 13). This approach was intended to confer specificity for cDNA-derived templates, as successful primer annealing would require the contiguous exon junction created following mRNA splicing. In contrast, genomic DNA templates retain intronic sequence between adjacent exons, disrupting the primer binding site and thereby preventing amplification. In the initial design, approximately half of the reverse primer sequence annealed to one exon, while the remaining half annealed to the neighboring exon.

These novel primers were then tested using a standard PCR and electrophoresis gel (Figure 14). In the cDNA samples, the novel primers effectively eliminated the higher molecular weight gDNA-associated bands observed with the original primer sets for most genes, demonstrating improved specificity. The only apparent exception was *dlx2a*, which showed limited amplification; however, this target had consistently exhibited minimal gDNA contamination with the original primers and was therefore considered less problematic. Examination of NRT controls, however, revealed that amplification of gDNA-derived products still occurred across several targets. Subsequent troubleshooting suggested that this residual amplification resulted from partial primer annealing, whereby the front portion of the reverse primer was sufficient to initiate extension despite incomplete binding across the intended exon–exon junction (Figure 13).

These findings indicated that the exon–exon junction strategy was fundamentally sound, but required further refinement to prevent incomplete primer binding. Accordingly, the reverse primers were redesigned such that only a small number of nucleotides annealed to the upstream exon, while the majority of the sequence annealed to the downstream exon. This asymmetric configuration reduced the likelihood of partial annealing to genomic templates while preserving efficient amplification of cDNA. These redesigned primers constituted the final optimized primer sets used for subsequent qPCR analyses (Table 4).

1st Generation Primers

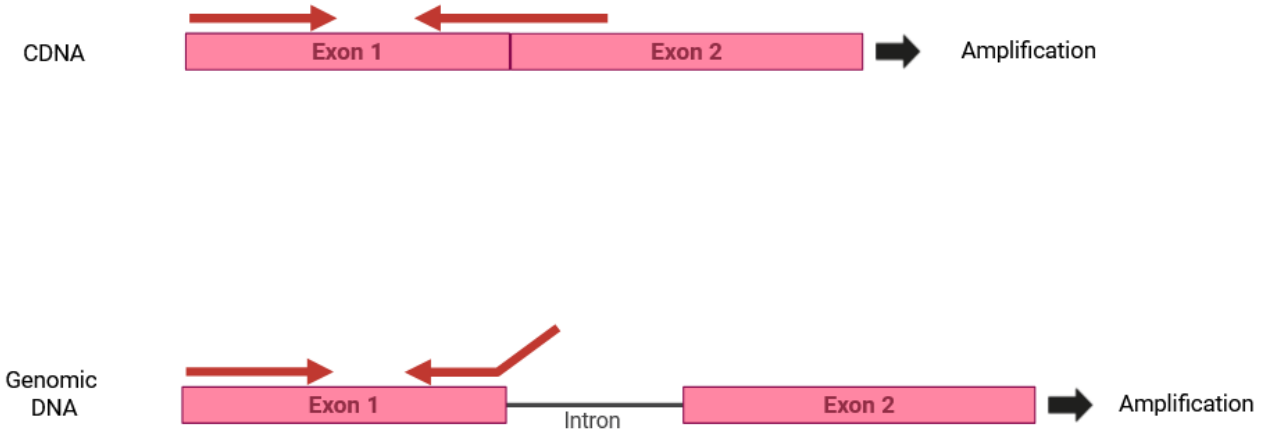

2nd Generation Primers

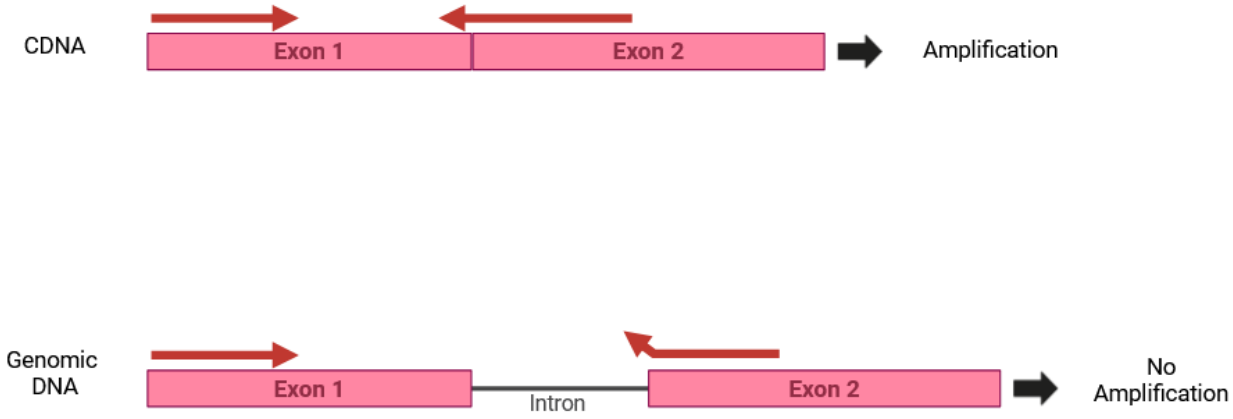

Figure 14. Schematic representation of novel primer design strategies for selective cDNA amplification. Exons are represented by pink boxes, intronic regions by black lines, and primer binding sites by red arrows. Primers were designed to span exon–exon junctions in order to preferentially amplify reverse-transcribed cDNA while minimizing amplification of contaminating gDNA. The upper panel illustrates the first generation of primer designs, in which approximately half of the primer sequence annealed to one exon and the remaining half to the adjacent exon however partial primer annealing still occurred, resulting in nonspecific amplification of genomic DNA. The lower panel depicts the second-generation primer design, in which only a few base pairs anneal to one exon while the majority of the primer sequence binds to the adjacent exon. This asymmetric design substantially improved specificity and effectively eliminated detectable gDNA amplification.

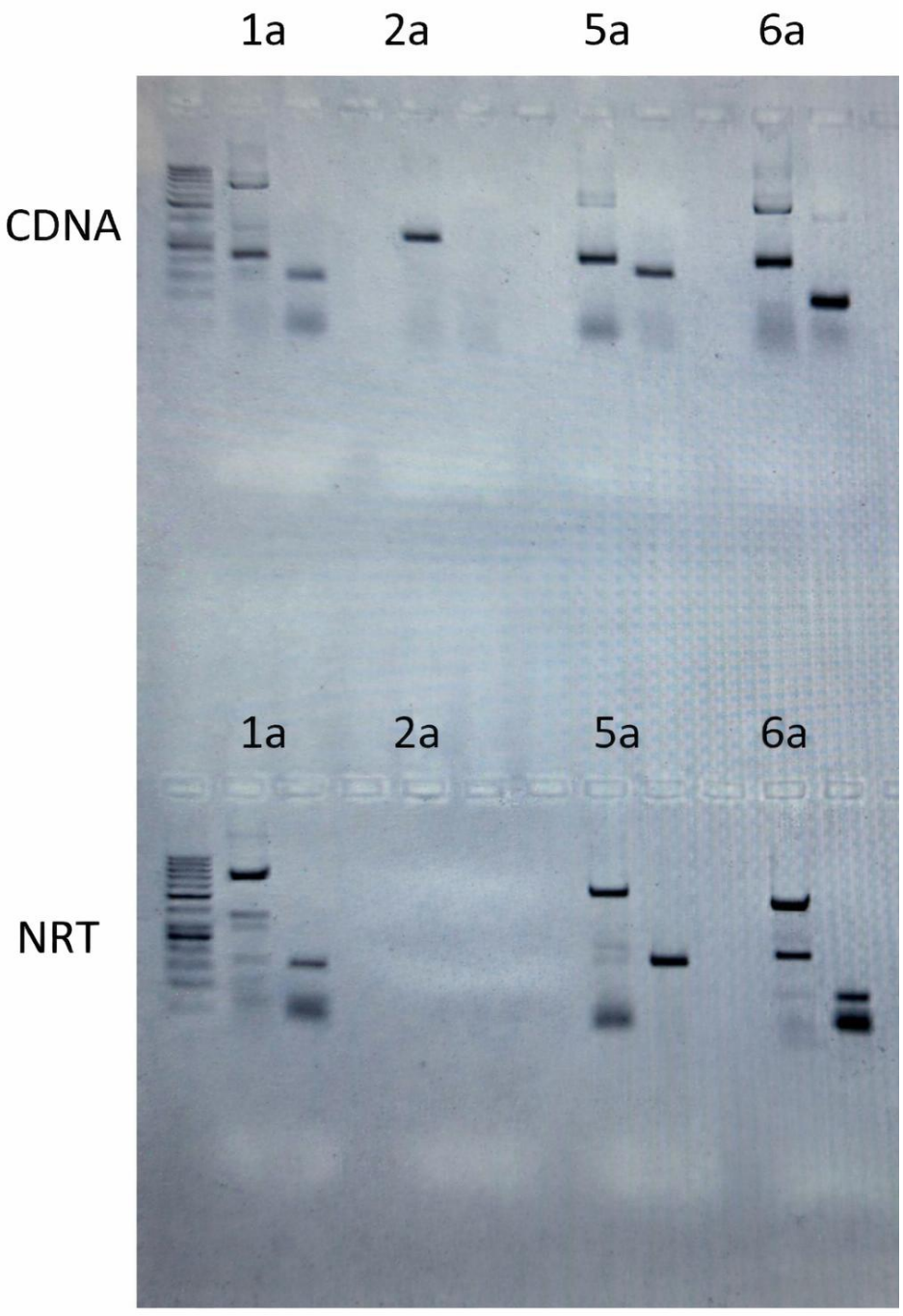

Figure 15. Diagnostic gel comparing the old QPCR primers to their Novel counterparts in CDNA and NRT samples. Agarose gel electrophoresis of PCR products generated using standard PCR conditions matching the annealing temperatures and cycling parameters used for subsequent qPCR analyses. Templates consisted of cDNA synthesized using the Bio-Rad iScript reverse transcription kit from RNA isolated by TRIzol extraction. The upper row contains reactions performed with cDNA templates, while the lower row contains NRT samples. For each gene analyzed, the left lane represents amplification using the original primer set, whereas the right lane represents amplification using the novel primer design illustrated in Figure 13.

Target Gene	Primer Sequences
dlx1a	F1: TACCAGAGAGTCTAAACAGCC R4: GTCCACTTCTAGACCAAAGTC
dlx2a	F1: CATTCGAACCAGATTACCTCC R3: GTCCAATTTTAGACCAAGGTC
dlx5a	F1: ACCCCTATAGAGTTAGACTGC R5: TCGGCTGTTTCTTTTTCTTGC
dlx6a	F1: ATTTACTAAGCCCACCTTCC R4: CTGTTGTTTTCTGCTGTTCTG

Table 5.Optimized *dlx* primers for QRTPCR in 5' to 3' orientation.

3.2.2 qPCR primer validation

The objective of this experiment was to validate an optimized qPCR protocol for the quantification of *dlx* gene expression in zebrafish. To achieve this, newly designed primer sets were tested on cDNA synthesized from whole-embryo RNA collected at 24 hpf. A central aim of this validation was to determine whether these primers effectively minimize gDNA contamination, thereby enabling accurate and reliable measurement of *dlx* transcript levels. As shown in Figure 15, these optimization efforts were successful: all targeted *dlx* genes exhibit amplification within a cycle range of approximately 20–30, while any signal observed in negative controls occurs substantially later, beyond 30 cycles. This temporal separation indicates that nonspecific amplification or residual contamination does not contribute to the experimental signal. These results represent a marked improvement over earlier qPCR attempts, in which simultaneous amplification of gDNA and cDNA precluded reliable quantification.

To further illustrate primer performance, Figure 16 presents a simplified analysis focusing on *dlx2a*. By reducing visual complexity, this figure more clearly demonstrates the specificity and reproducibility of amplification. Replicate samples show highly consistent amplification profiles, while both NRT and NTC reactions remain negative until late cycles, consistent with background fluorescence rather than true amplification. Collectively, these findings confirm that the optimized primer sets and protocol provide a robust and reliable framework for quantifying *dlx* gene expression in zebrafish. This methodological advancement establishes a strong foundation for future studies investigating the regulatory dynamics and functional roles of *dlx* genes in development and regeneration.

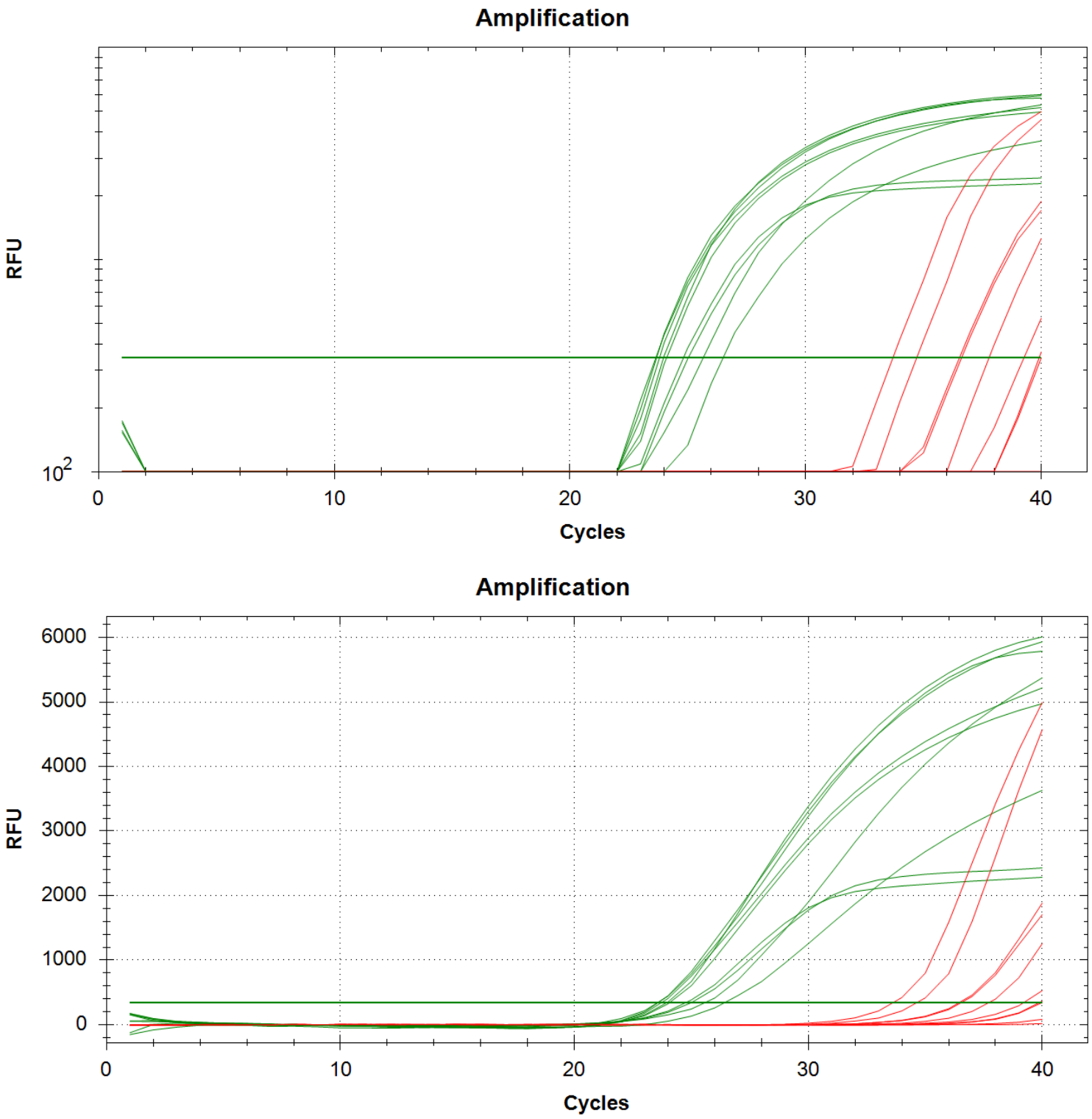

Figure 16. qPCR primer validation results. Primer sets targeting four *dlx* genes (*dlx1a*, *dlx2a*, *dlx5a*, and *dlx6a*) were assessed alongside the housekeeping gene *rpl13a*. Amplification curves for experimental samples are shown in green, while negative controls (NRT and NTC) are shown in red. Compared to earlier optimization attempts, the *dlx* targets demonstrate robust amplification between approximately 20–30 cycles, whereas nonspecific amplification in control reactions occurs at substantially later cycles, supporting improved primer specificity for cDNA and the absence of detectable contamination. The data is presented in both linear (top) and logarithmic (bottom) scales.

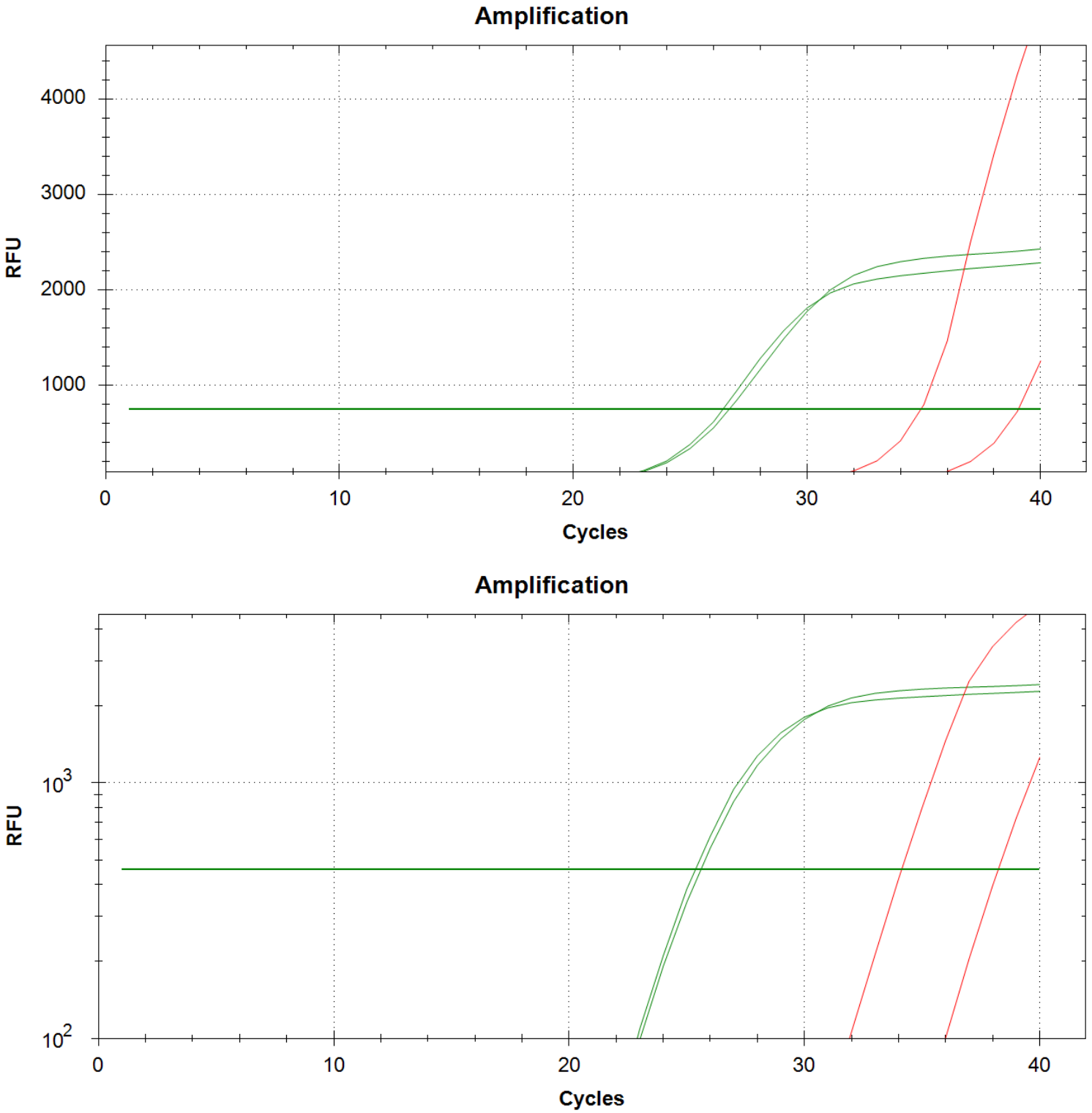

Figure 17. qPCR primer validation results for *dlx2a*. Amplification curves for experimental samples are shown in green, while negative controls (NRT and NTC) are shown in red. This simplified representation, focusing on a single gene, improves clarity relative to Figure 18 and more clearly demonstrates the absence of contamination. Data are presented on both linear (top) and logarithmic (bottom) scales.

3.2.3 Bioinformatic analysis reveals baseline *dlx* expression patterns

The purpose of this section is to leverage existing RNA-seq datasets to establish a baseline profile of *dlx* gene expression patterns. Defining this reference framework provides an essential point of comparison for subsequent qPCR-based analyses, enabling more informed interpretation of changes in transcript abundance. However, it is important to recognize a key limitation of this approach: the RNA-seq data utilized here are derived specifically from cells within the ventral forebrain, whereas the qPCR experiments described in this study are performed on whole-larval RNA extracted from zebrafish. As a result, direct comparisons must be made with caution, as spatially restricted expression patterns observed in the RNA-seq dataset may be diluted or obscured in whole-organism measurements.

Analysis of the DanioCell dataset, restricted to cells isolated from the zebrafish ventral forebrain, revealed distinct yet overlapping developmental expression profiles among the *dlx* paralogs (*dlx1a, dlx2a, dlx5a,* and *dlx6a*) across sequential embryonic and larval timepoints ranging from 14–21 hpf to 120 hpf (Figure 17). In this visualization, dot size represents the proportion of ventral forebrain cells expressing each transcript, while color intensity reflects mean expression level. *dlx1a* displayed strong and highly consistent expression throughout all examined stages, with a large proportion of expressing cells from early embryogenesis (14–21 hpf) through later larval development (120 hpf), suggesting a sustained role in ventral forebrain patterning and neuronal differentiation. A similarly robust pattern was observed for *dlx5a*, which maintained broad expression from 24–34 hpf onward and remained highly expressed through later stages, consistent with prolonged involvement in developmental specification or

maintenance of neuronal identity. In contrast, *dlx2a* showed its highest expression during earlier developmental windows, particularly between 14–21 hpf and 48–58 hpf, after which both transcript abundance and the proportion of expressing cells progressively declined from 60 hpf to 120 hpf. This pattern suggests that *dlx2a* may function more prominently during early neurogenesis and initial ventral forebrain regionalization. Among the genes analyzed, *dlx6a* exhibited the weakest and most restricted expression profile, with relatively few positive cells detected across all timepoints and lower overall transcript levels. Expression of *dlx6a* increased modestly during intermediate stages, particularly between 36–46 hpf and 72–82 hpf, before remaining low but detectable through 120 hpf, indicating a potentially specialized or cell type-restricted role. Collectively, these findings support a model in which zebrafish *dlx* genes exhibit partially redundant yet temporally specialized functions in ventral forebrain development.

These findings are broadly consistent with the current understanding of *dlx* gene function during GABAergic neuron development. Previous studies have shown that *dlx1* and *dlx2* are strongly expressed during early developmental stages, where they play key roles in initiating interneuron migration of GABAergic neurons from the ventral forebrain. The present analysis supports this model, as *dlx2a* expression was highest during early embryogenesis before gradually declining at later stages. In contrast, *dlx5a* displayed sustained and elevated expression during later developmental windows, consistent with reports that *dlx5/6* paralogs function downstream of *dlx1/2* to support neuronal maturation and maintenance of interneuron identity. Together, these temporal expression profiles reinforce the proposed sequential activity of the *dlx* gene network during forebrain development.

Most notably, *dlx6a* exhibited substantially lower overall expression than the other analyzed paralogs across all examined timepoints. This comparatively weak and restricted expression pattern may suggest that *dlx6a* plays a more limited or specialized role in zebrafish brain development than previously assumed, at least within the ventral forebrain. This interpretation is further supported by the present in situ hybridization results, which detected no significant differences in SST^{+} neuron counts between wildtype and *dlx6a* knockout animals. While absence of phenotype does not necessarily indicate lack of function, the combined transcriptional and histological data suggest that *dlx6a* may be less critical for the development of certain GABAergic interneuron subtypes than other members of the gene family.

Despite the insights gained from this RNA-sequencing dataset, these findings also highlight the need for targeted qPCR experiments. The DanioCell data were generated exclusively from wildtype animals and therefore cannot address how loss of individual *dlx* genes alters expression of the remaining paralogs. Performing qPCR on the available mutant lines would provide a more direct assessment of compensatory transcriptional responses, regulatory interactions, and the functional consequences of the clustered genomic organization of the *dlx* family. Such analyses would substantially expand our understanding of how these transcription factors interact to coordinate zebrafish forebrain development.

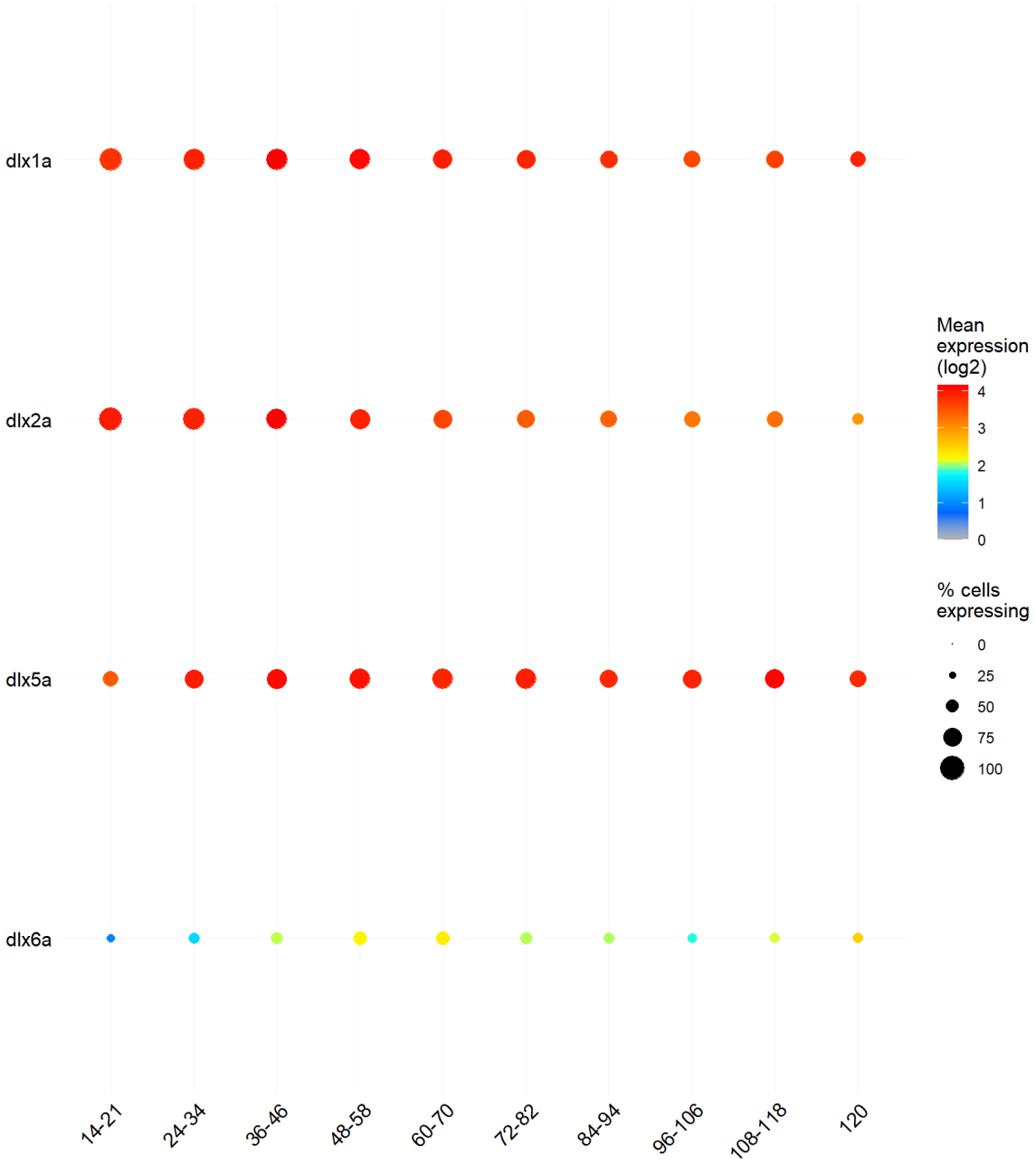

Figure 18. Developmental expression of zebrafish *dlx* paralogs in ventral forebrain cells from the DanioCell dataset. Dot plot illustrating the temporal expression profiles of *dlx1a, dlx2a, dlx5a,* and *dlx6a* in cells derived from the zebrafish ventral forebrain across developmental stages ranging from 14–21 hpf to 120 hpf. Dot size represents the percentage of cells expressing each gene, while dot color indicates mean transcript expression level (log2 scale).

4. Discussion

4.1 How does loss of *dlx* impact the development of GABAergic interneurons

This section presents the results of the histological analysis of GABAergic neuron populations in the zebrafish brain, alongside a critical evaluation of its methodological limitations. It further outlines potential avenues for improvement, including the application of whole-brain clearing approaches and the use of more optimized antibody selection strategies to enhance resolution, specificity, and overall interpretability of future experiments.

4.1.1 Impact of *dlx* mutations on GABAergic interneurons

Beginning with our SST staining. Our SST staining produced consistent and biologically interpretable results. Here, *dlx5a* and *dlx1a* mutants exhibited the most pronounced reductions in SST^+ neuron numbers, while *dlx2a* mutants showed a more modest decrease that did not reach statistical significance. These findings align with previous studies demonstrating a central role for *dlx1/2* gene clusters in the differentiation and specification of GABAergic interneuron subtypes (Anderson et al., 1997c; Cobos et al., 2007). Interestingly, deletion of *dlx6a* did not produce a measurable change in SST neuron numbers. This observation is supported by our RNA-seq analysis, which indicates that *dlx6a* expression remains comparatively low in the zebrafish brain throughout development. Taken together, these results suggest that *dlx6a* may

play a more limited or redundant role in SST interneuron specification than initially hypothesized.

Secondly, analysis of CR interneurons revealed a significant reduction in both *dlx5a* and *dlx2a* mutant lines, supporting their involvement in the development of this neuronal subtype. However, as only these two genotypes were examined in detail, broader comparisons across the *dlx* gene family remain limited. It is therefore unclear whether *dlx6a* contributes meaningfully to CR interneuron development or whether its apparent lack of effect in SST populations extends to other GABAergic subtypes. Additional experiments incorporating a wider range of mutants will be necessary to resolve this question and to further clarify the relative contributions of individual *dlx* genes to interneuron diversification.

Finishing with the PV immunostaining, it is important to interpret our results with caution. We observed a statistically significant reduction in PV+ cell counts in the TeO across all mutant lines with the exception of *dlx2*. However, although statistically significant differences were observed, there remain clear technical limitations that undermine confidence in the absolute cell counts. Despite optimization efforts yielding consistent staining with high signal-to-noise ratios, variability between samples remains substantial. Notably, we observe up to a five-fold difference in PV^+ cell counts between *dlx2a* and *dlx5a* wild-type controls—groups for which variation would be expected to remain within approximately 10% under ideal conditions. This level of inconsistency suggests that the current staining protocol does not fully capture the true population of PV-expressing interneurons in the zebrafish brain.

4.1.2 Potential factors influencing low PV cell count numbers

Although effort was devoted to optimizing the immunohistochemistry protocol for PV staining, resulting in a method that consistently produced detectable PV labeling with low background signal and good overall contrast, several important limitations remained evident. Most notably, PV-positive cell counts displayed unexpectedly high variability among wildtype specimens, whereas counts within genetically similar control animals would be expected to remain comparatively consistent under standardized experimental conditions. In addition, the total number of PV-positive neurons identified was markedly lower than the counts obtained for SST and CR populations. This observation is difficult to reconcile with the broader literature on inhibitory neuron diversity, in which PV-expressing interneurons are generally considered one of the most abundant GABAergic subclasses, particularly in forebrain circuits where they often represent a major proportion of inhibitory neurons. While exact proportions vary by species and anatomical region, the comparatively low PV counts observed in the present study suggest that the staining likely underestimated the true abundance of this neuronal population.

Although several biological and technical explanations could account for this discrepancy, the most plausible cause is antibody incompatibility or incomplete antigen recognition. The antibody used in this study, Swant PV235, is reported by the manufacturer to be suitable for zebrafish tissue and has previously been used within our laboratory. However, staining presented in prior work using this reagent appeared relatively weak, with low apparent PV cell numbers and modest signal intensity, findings consistent with the present results(Solek et al., 2017). By contrast, a paper using an alternative antibody, Swant PV27, reported

substantially stronger and more convincing PV labeling in the zebrafish brain(Kenney et al., 2021). A key distinction between these reagents is their immunological design: PV235 is a monoclonal antibody raised in mouse, whereas PV27 is a polyclonal antibody raised in rabbit.

This difference may be highly relevant in the context of zebrafish neurobiology. Monoclonal antibodies recognize a single epitope on the target protein and are typically favored for their specificity, low background staining, and reproducibility. However, this same specificity may become a limitation when working in species such as zebrafish, which possess 9 parvalbumin-related genes as a result of teleost genome duplication events(Friedberg, 2005). These paralogs may encode proteins with sequence divergence at the epitope recognized by PV235, potentially restricting detection to only a subset of PV-expressing neurons. In contrast, polyclonal antibodies consist of a mixture of immunoglobulins recognizing multiple epitopes on the target antigen. This broader binding capacity may allow improved recognition of several zebrafish parvalbumin proteins simultaneously, thereby producing stronger staining and a more accurate representation of total PV-positive neuronal populations. +However, it is important to note that when examining the amino acid sequence of the 9 zebrafish PV isoforms, a very high degree of similarity remains, this suggest that other factors might also be influencing our low cell counts.

Taken together, these observations suggest that the low and variable PV counts obtained in the present study likely reflect incomplete immunodetection rather than true biological scarcity of PV interneurons. Future work comparing PV235 and PV27 directly on matched zebrafish tissue would be valuable in determining the most reliable strategy for quantifying PV neurons in this model system.

Another potential strategy to address this issue is to perform FISH targeting each of the 9 parvalbumin transcripts. While immunohistochemistry is generally preferred from a biological standpoint, as it directly detects protein levels rather than mRNA, FISH may represent a more reliable approach for assessing parvalbumin expression in this context.

Our lab's FISH protocol has been shown to be highly robust, producing strong, highly specific signal with minimal background, resulting in clear cellular resolution of expressing populations. Importantly, this approach circumvents the persistent issue of antibody incompatibility that can significantly compromise IHC-based detection of parvalbumin. Given the variability observed with our PV antibody, this represents a meaningful technical advantage.

In addition, FISH also offers substantial practical benefits. Antibodies suitable for reliable IHC cannot be produced in-house and are often prohibitively expensive, making iterative optimization and troubleshooting costly and time-consuming. In contrast, FISH probes can be designed and synthesized in-house at relatively low cost, providing a more flexible and scalable approach. Taken together, these advantages suggest that FISH may not only resolve current technical limitations but also offer a more efficient and reproducible method for assessing PV neuron populations in future experiments. However, it is important to note that performing staining for all nine parvalbumin-related genes would represent a substantial experimental undertaking, requiring significant time and resources. As such, this approach would likely be best reserved as a last-resort strategy should alternative methods fail to produce sufficiently reliable or interpretable results.

4.1.3 Improvements to GABAergic neuron quantification

Although neuronal quantification using immunohistochemistry and fluorescent in situ hybridization on tissue sections remains a well-established and widely validated methodology, it is not without important scientific and practical limitations. While these approaches have proven highly valuable for assessing spatial distribution and relative abundance of neuronal populations, they do not necessarily represent the most precise means of quantification. One of the principal limitations is the inherent variability introduced during tissue sectioning and sample comparison. Even with standardization of orientation, embedding, and sectioning protocols, it is difficult to ensure that corresponding sections from different specimens represent the exact same anatomical position within the brain. Minor differences in rostrocaudal level or section angle may result in comparisons being made between slightly different regions, potentially influencing observed cell counts. Although this issue is mitigated by analyzing multiple sections spanning the region of interest across numerous biological replicates, such variability cannot be entirely eliminated.

Additional sources of error arise from the technical demands of microtomy itself. Consistency in section thickness, tissue integrity, and preservation of morphology depends heavily on a researcher's skill and precision. Variations in section quality can reduce staining consistency, obscure anatomical boundaries, or compromise accurate identification of labeled cells. Beyond these technical considerations, section-based methodologies are also highly labor intensive. Tissue processing, embedding, sectioning, staining, imaging, and manual quantification require substantial time and effort, greatly increasing the overall duration of

experiments. Furthermore, because variability is relatively high, larger sample sizes are often necessary to achieve sufficient statistical power. This consequently increases the number of animals required for experimentation, raising both financial costs and ethical considerations regarding animal use, which should be minimized whenever possible.

These limitations do not diminish the value of section-based histological approaches, which have been used reliably for decades and remain indispensable for many forms of neuroanatomical analysis. However, they do emphasize that such methods are not inherently free from variability or bias. Recognition of these shortcomings is important when interpreting results and when considering complementary or alternative methodologies that may improve precision, throughput, and experimental efficiency.

In recent years however a novel method for brain staining and imaging has been popularized in the scientific community that being whole brain clearing and staining. Tissue clearing methods render biological tissue optically transparent while preserving fluorescent labeling, allowing intact brains to be imaged in three dimensions using confocal, light-sheet, or optical projection tomography platforms. This approach is particularly well suited to zebrafish, whose relatively small brain size makes complete clearing and whole-organ imaging technically feasible. Several studies have demonstrated successful clearing of juvenile and adult zebrafish brains while maintaining structural integrity and fluorescent signal, enabling visualization of labeled cells throughout the entire brain rather than within isolated tissue sections (K. Wang et al., 2023).

From an experimental perspective, whole-brain staining offers several major advantages over conventional slide-based quantification. Most importantly, it eliminates sampling error introduced by sectioning, as the entire brain can be analyzed rather than a subset of representative slices. This approach removes uncertainty introduced during tissue sectioning, as well as variability arising from differences in section quality, and allows for direct quantification of total neuronal populations within the intact brain. It also enables researchers to visualize the distribution of neuronal populations across the entire brain at a glance, potentially revealing phenotypes that may have been overlooked in section-based analyses due to the need to focus on a limited region of interest. In addition, three-dimensional visualization of the intact brain enables researchers to examine the spatial relationships between cells, providing a more comprehensive understanding of neuronal migration, clustering, and regional organization—information that is often lost or fragmented when analyzing two-dimensional tissue sections alone. In a 2018 study, Lindsey et al. used whole-brain clearing techniques to reconstruct the adult zebrafish brain at near-cellular resolution, allowing visualization of proliferative zones and neuronal morphology throughout the entire brain (Lindsey et al., 2018). A whole-brain dataset of this nature would be particularly valuable in the context of the *dlx* gene family, which plays a central role in regulating GABAergic neuron specification and migration. Applied to the mutant lines used in my thesis such an approach could provide far greater insight into the individual functions of each *dlx* gene and the broader neuroanatomical consequences of their loss than would be possible through conventional sectioning and regional cell counts alone.

Whole-brain approaches can also reduce labor and improve experimental efficiency. Traditional histology requires fixation, embedding, sectioning, staining, and manual counting

across many slides, each step introducing time demands and technical variability. In contrast, once optimized, whole-mount staining and clearing pipelines allow a single specimen to be processed and imaged intact, and can generate reusable digital datasets that can be reanalyzed computationally. Automated image analysis software can further quantify labeled cells or fluorescence intensity across entire brain regions, reducing observer bias and increasing throughput. Because variability may be lower and complete datasets are obtained from each animal, fewer specimens are required to achieve statistical power, helping reduce animal use.

Despite these advantages, whole-brain clearing is not without limitations. Antibody penetration into dense adult tissue, autofluorescence, long incubation times, and the need for specialized imaging systems, and computational tools remain practical barriers. Another limitation is a loss of direct quantification, although recent studies are able to image whole brain staining with exceptional detail, they do not quite reach the resolution necessary to count individual cells, instead relying on pixel counts as a stand in. However, pixel counts still provide a reliable method of quantification and further developments in brain clearing and imaging will continuously improve the resolution as time goes on. Continued refinement of zebrafish-specific clearing methods suggests that whole-brain staining represents a powerful future direction for neurodevelopmental studies. For projects investigating altered interneuron populations in *dlx* mutants, this methodology could provide more comprehensive and anatomically accurate quantification than conventional section-based approaches while simultaneously revealing large-scale changes in brain organization.

4.1.4 GABAergic neuron quantification in the regenerating zebrafish brain

One of the most significant advantages of using zebrafish as a model for neurobiological research, particularly when compared to mammalian systems, is their remarkable capacity for central nervous system regeneration. Unlike mammals, in which neurogenesis is largely restricted to discrete regions and regenerative potential is limited, teleost fish such as zebrafish retain widespread neurogenic activity throughout adulthood. This persistent plasticity enables regeneration following injury and provides a framework for studying mechanisms of brain repair that are largely inaccessible in other vertebrate models. Previous work conducted in our laboratory using a mechanical lesion of the brain demonstrated that members of the *dlx* gene family are strongly implicated in this regenerative response. In particular, elevated expression of the *dlx5/6* bigene cluster was observed in regions adjacent to the damaged tissue, suggesting an active role in promoting neuronal regeneration, with evidence pointing toward *dlx5* as a potential key driver of this process (Mendes et al., 2020b). However, this study was only performed on WT fish, therefore it would be pertinent to observe how this regeneration is impacted in our mutant lines.

Addressing this gap represents an important direction for future research. By leveraging the existing *dlx* mutant lines, it would be possible to systematically assess how loss of individual *dlx* genes impacts the zebrafish brain's ability to regenerate following injury. Repeating lesion-based regeneration assays in these knockout backgrounds would allow for precise dissection of gene-specific roles, including whether particular *dlx* paralogs exert disproportionately large effects on regenerative outcomes or whether compensatory mechanisms mitigate the impact of

single-gene deletions. Such experiments would clarify the essential roles each individual *dlx* gene plays during neuroregeneration.

This approach could be further strengthened through integration with whole-brain clearing and three-dimensional imaging techniques mentioned previously. Traditional section-based histology, while informative, inherently limits spatial resolution and may obscure dynamic cellular processes occurring across the intact brain. In contrast, whole-brain clearing enables comprehensive visualization of cellular organization and migration within an undisturbed three-dimensional context. This is particularly relevant in the context of regeneration, where GABAergic interneurons are expected to migrate through complex spatial environments to repopulate damaged regions. Applying whole-brain imaging to regenerating brains at multiple post-lesion time points would therefore allow for detailed tracking of neuronal migration and integration, providing insights into both the timing and spatial coordination of repair processes. Coupling this with molecular markers for GABAergic identity and *dlx* expression would yield a more complete picture of how these genes influence not only cell fate specification but also the physical reconstruction of neural circuits following injury.

4.2 Optimizing *dlx* gene quantification via qPCR

The objective of the second part of this thesis was to develop and optimize a robust qPCR-based protocol for quantifying *dlx* gene expression in zebrafish. Achieving this required overcoming several technical challenges inherent to the *dlx* gene family, including their

relatively low expression levels and compact genomic structure characterized by small intronic regions. Through our optimization efforts we found that these features complicate primer design and increase the likelihood of genomic DNA amplification, thereby reducing assay specificity and sensitivity. Consequently, optimization was necessary to establish conditions that enable accurate quantification of *dlx* transcripts.

4.2.1 Primer design for lowly transcribed small genes

In the course of optimizing *dlx* gene quantification by qPCR in zebrafish, a primary technical challenge encountered was the persistent presence of gDNA contamination. Despite our initial primer set being designed to span distinct exons, a conventional strategy used to minimize gDNA amplification, persistent gDNA contamination was observed throughout our experiments. This is due to the unique nature of the *dlx* gene family characterized by small transcript length and even smaller intronic regions. Initial attempts to mitigate this issue relied on treatments aimed at degrading residual gDNA; however, while these approaches were partially effective, they resulted in a substantial loss of total RNA yield. Given the already low expression levels of *dlx* transcripts, this reduction proved detrimental, as it shifted amplification to later cycles where signal became difficult to distinguish from background fluorescence and nonspecific amplification. As such, an alternative strategy was required to minimize gDNA interference without compromising RNA integrity.

To address this, a series of novel primer designs were developed to preferentially amplify cDNA, The first generation of primers was designed to span exon–exon junctions, a

common strategy intended to prevent amplification of intron-containing genomic sequences. However, these primers proved insufficiently specific. Due to their symmetric design—where approximately half of the primer sequence annealed to each exon—it was possible for partial binding to occur on gDNA templates, leading to unintended amplification. Consequently, a second generation of primers was developed to overcome this limitation. In this iteration, primers were designed such that only a minimal number of nucleotides (approximately 2–4 base pairs) annealed to one exon, with the majority of the sequence binding to the adjacent exon. This asymmetric design significantly reduced the likelihood of partial annealing to gDNA, thereby improving specificity for cDNA targets and effectively minimizing contamination without sacrificing RNA yield. This refinement ultimately marked the successful conclusion of the qPCR optimization process.

Beyond its immediate application to the *dlx* gene family, this work highlights several important considerations for qPCR assay development more broadly. In particular, it underscores the importance of tailoring primer design strategies to the specific genomic architecture of the target genes, especially in cases involving low transcript abundance and compact intronic regions. These insights may therefore prove broadly applicable to similar experimental contexts, providing a useful framework for optimizing qPCR-based gene expression analyses in other challenging systems.

4.2.2 Potential qPCR experiments

qPCR analyses could not be completed within the scope of this study; instead, efforts were focused on the successful design and optimization of primers targeting the *dlx* gene family. Nevertheless, the application of qPCR to these targets represents a promising avenue for future investigation into the functional significance of the organization of *dlx* genes. Given that *dlx* genes are expressed with overlapping spatial and temporal expression domains, qPCR offers a sensitive and quantitative method capable of detecting subtle changes in transcript abundance that may not be evident through phenotypic analysis alone. Due to *dlx* genes convergent transcription and shared regulatory elements characteristic of these bigene clusters we hypothesize that there is strong potential for compensatory transcriptional responses among paralogs. Indeed, prior studies have demonstrated that loss of *Dlx2* results in reduced activity of the intergenic enhancer *I56i*, leading to decreased *Dlx5/6* expression (Zerucha et al., 2000). Additionally, the deletion of a second enhancer, *I56ii*, similarly reduces *Dlx5/6* levels but is accompanied by an increase in *Dlx1* expression, indicative of compensatory regulation (Fazel Darbandi et al., 2016). More recent work in zebrafish has expanded on these findings, showing that simultaneous deletion of both *i56i* and *i56ii* enhancers results in reduced *dlx5/6* expression alongside a concurrent upregulation of *dlx1*, further supporting the existence of complex cross-regulatory mechanisms within the *dlx* network (Yu et al., 2021). Collectively, these findings underscore the intertwined nature of *dlx* gene regulation; however, a comprehensive understanding of this system will require systematic analysis of how loss of individual *dlx* genes and their associated enhancers influences the expression of all other *dlx* family members. Such studies have been challenging in the mouse

model due to early embryonic and post natal lethality, but this limitation is largely overcome in zebrafish models. As such, the availability of a method to quantify dlx transcripts, as developed here. provide a valuable tool for future work aimed at dissecting compensatory transcriptional dynamics and elucidating the regulatory architecture governing *dlx* gene expression.

A particularly interesting mutant for our understanding of *dlx* regulation would be the *inter56* mutant line which is a double KO of both *i56i and i56ii* intergenic enhancers found within the *dlx5/6* bigene cluster. As mentioned previously these enhancers are thought to mediate cross-regulatory interactions between *dlx* proteins themselves. Additionally, comparative studies across vertebrates have shown that these intergenic domains are deeply conserved and function as enhancers, highlighting their functional importance in maintaining overlapping expression domains (Ghanem et al., 2003b). Performing qPCR on this mutant line would allow the understanding of its role in maintaining coordinated gene expression between *dlx5* and *dlx6*. Furthermore, such an approach could determine whether enhancer loss leads to asymmetric effects on the paired genes, thereby clarifying whether shared enhancers act uniformly or exhibit gene-specific biases. Collectively, integrating qPCR analyses of *dlx* mutants with deletion of conserved intergenic enhancers represents a powerful strategy to elucidate the regulatory architecture of the *dlx* gene family and to better understand how genomic organization, enhancer sharing, and compensatory transcriptional networks interact to govern their expression and vertebrate forebrain development.

4.2.3 Using gene Knock-ins to further our understanding of the dlx gene family

Another future direction for dissecting the regulatory logic of the *dlx* gene family lies in the application of targeted gene knock-in strategies to experimentally manipulate the composition of *dlx* bigene clusters. The *dlx* genes are organized as convergently transcribed paralogous pairs (e.g., *dlx1/2* and *dlx5/6*) that share intergenic regulatory elements and exhibit overlapping expression domains, a genomic configuration that is highly conserved across vertebrates and thought to underpin coordinated gene regulation. While previous loss-of-function studies have highlighted redundancy and cross-regulation within this family, they do not fully resolve whether these relationships are driven primarily by protein function, genomic context, or shared cis-regulatory architecture. By contrast, knock-in approaches—specifically replacing one *dlx* gene within a bigene cluster with another paralog (for example, substituting *dlx5* with *dlx6* within the *dlx5/6* locus and vice versa) would allow for direct interrogation of whether gene function is interchangeable when placed under the control of an alternative regulatory environment. Such strategies have been enabled by advances in targeted genome editing technologies, particularly CRISPR-Cas9, which permit precise locus-specific modifications in model organisms including zebrafish.

This experimental design would provide critical insight into the extent to which *dlx* gene expression and function are dictated by local genomic context versus intrinsic protein properties. If the function of a substituted knock-in gene is fully preserved despite being expressed under the regulatory environment of a different dlx locus, this would support the hypothesis that spatial and temporal expression patterns driven by shared enhancers and are

the primary determinants of *dlx* gene function. Conversely, if the knock-in fails to rescue the phenotype or results in altered developmental outcomes despite appropriate expression, this would suggest that the specific protein sequence and intrinsic functional properties of individual *dlx* transcription factors also play a critical role. Prior studies have demonstrated that intergenic enhancers within *dlx* bigene clusters, such as I56i and I56ii, are capable of driving highly specific expression patterns and mediating cross-regulatory interactions among *dlx* genes (Fazel Darbandi et al., 2016; Ghanem et al., 2003b; Zerucha et al., 2000). Furthermore, the evolutionary conservation of this clustered organization, including preserved enhancer function despite sequence divergence, underscores the importance of genomic context in maintaining coordinated expression. However, these studies stop short of experimentally decoupling protein sequence from genomic position—an important gap that knock-in approaches are uniquely suited to address.

Beyond testing regulatory sufficiency, such knock-in models could also reveal previously unappreciated aspects of compensatory dynamics within the *dlx* network. For instance, replacing one paralog with another may disrupt established feedback loops or alter competitive interactions for shared enhancers, thereby exposing how dosage balance and enhancer occupancy contribute to stable gene expression. When combined with downstream analyses such as qPCR, in situ hybridization, and immunohistochemistry, these models would enable a comprehensive assessment of how genomic organization, enhancer sharing, and protein sequence converge to regulate *dlx*-mediated developmental processes. Importantly, the use of zebrafish circumvents limitations encountered in mammalian systems, such as early embryonic lethality, allowing for simultaneous analysis of both developmental and regenerative

phenotypes. Collectively, the implementation of gene replacement strategies within *dlx* bigene clusters represents a highly informative approach to unraveling the principles governing their genomic organization and functional coordination.

It is important to acknowledge that the generation of stable knock-in lines in zebrafish remains technically challenging, with no universally reliable or high-efficiency methodology currently established. Although advances in CRISPR-Cas9–mediated genome editing have significantly improved the feasibility of targeted modifications, precise knock-in events—particularly those involving large genomic insertions or locus replacement—continue to suffer from low efficiency.

In light of these limitations, an alternative—albeit less controlled—approach could still provide valuable insight into *dlx* genomic organization. During CRISPR-Cas9–mediated editing, it is not uncommon for targeted sequences to reintegrate into the genome in an inverted orientation. If such an event were to occur across an entire *dlx* bigene cluster and be successfully isolated to generate a stable line, it would offer a unique opportunity to examine how inversion of genomic context influences gene expression and regulatory coordination. This strategy could help elucidate the extent to which the spatial orientation of *dlx* genes contributes to their coordinated regulation. However, a critical limitation of this approach is that inversion would also affect the intergenic enhancer elements located between the paired *dlx* genes. Given that these enhancers are central to driving coordinated and region-specific expression, their inversion may disrupt normal regulatory interactions in ways that complicate interpretation. As a result, while such a model could yield informative phenotypes, care would be required in disentangling the effects of gene inversion from those arising due to altered enhancer function.

5 Conclusion

In conclusion, this study aimed to both investigate the effects of *dlx* gene deletions on GABAergic interneuron development and to develop an optimized protocol for *dlx* quantification via qPCR to support future molecular analyses of this gene family. Together, these complementary approaches provide both biological insight and methodological groundwork for advancing our understanding of the atypical organization and function of the *dlx* bigene clusters.

With respect to interneuron development, the results demonstrate that *dlx* paralogs contribute differentially to GABAergic subtype specification. While no definitive conclusions could be drawn regarding the impact of *dlx* deletions on parvalbumin expressing interneurons due to persistent variability and technical limitations in staining, more consistent patterns emerged for other subtypes. Notably, *dlx1a* and *dlx5a* were found to play major roles in the development of somatostatin expressing neurons, while *dlx2a* and *dlx5a* were shown to be important for calretinin interneuron populations.

In parallel, this work addressed the technical challenge of qPCR primer design for the *dlx* gene family. Despite significant obstacles due to their low expression and small intronic regions functional and optimized primer sets were successfully developed. These primers provide a valuable tool for future studies aimed at dissecting regulatory interactions within the *dlx* network, including how deletion of individual genes influences the expression of others and

how shared intergenic enhancers contribute to the maintenance and evolution of the characteristic bigene cluster arrangement.

Overall, this study establishes a strong foundation for future research. By combining histological analysis with validated molecular tools, this thesis offers both preliminary biological insights and the groundwork for continued investigation. Future work building on these findings will be well-positioned to more precisely define the regulatory architecture of the *dlx* gene family and to further elucidate its critical role in GABAergic brain development.

References

Anderson, S. A., Eisenstat, D. D., Shi, L., & Rubenstein, J. L. R. (1997a). Interneuron migration from basal forebrain to neocortex: Dependence on Dlx genes. *Science*, *278*(5337), 474–476. https://doi.org/10.1126/SCIENCE.278.5337.474/ASSET/7372E40D-0F9F-4ED4-9A0D-67743214189B/ASSETS/GRAPHIC/SE4075793004.JPEG

Bartos, M., Vida, I., Frotscher, M., Meyer, A., Monyer, H., Geiger, J. R. P., Jonas, P., & Heidelberg. (2002). Fast synaptic inhibition promotes synchronized gamma oscillations in hippocampal interneuron networks. *Proceedings of the National Academy of Sciences of the United States of America*, *99*(20), 13222–13227. https://doi.org/10.1073/PNAS.192233099/SUPPL_FILE/2330TABLE1.PDF

Briggs, J. P. (2002). The zebrafish: a new model organism for integrative physiology. *American Journal of Physiology. Regulatory, Integrative and Comparative Physiology*, *282*(1). https://doi.org/10.1152/AJPREGU.00589.2001

Burgess, H. A., & Burton, E. A. (2023). A Critical Review of Zebrafish Neurological Disease Models−1. The Premise: Neuroanatomical, Cellular and Genetic Homology and Experimental Tractability. *Oxford Open Neuroscience*, *2*, kvac018. https://doi.org/10.1093/OONS/KVAC018

Cauli, B., Zhou, X., Tricoire, L., Toussay, X., & Staiger, J. F. (2014). Revisiting enigmatic cortical calretinin-expressing interneurons. *Frontiers in Neuroanatomy*, *8*(JUN), 93014. https://doi.org/10.3389/FNANA.2014.00052/XML

Cho, K. K. A., Hoch, R., Lee, A. T., Patel, T., Rubenstein, J. L. R., & Sohal, V. S. (2015). Gamma rhythms link prefrontal interneuron dysfunction with cognitive inflexibility in Dlx5/6(+/-) mice. *Neuron*, *85*(6), 1332–1343. https://doi.org/10.1016/J.NEURON.2015.02.019

Cobos, I., Borello, U., & Rubenstein, J. L. R. (2007). Dlx transcription factors promote migration through repression of axon and dendrite growth. *Neuron*, *54*(6), 873–888. https://doi.org/10.1016/J.NEURON.2007.05.024

Cobos, I., Calcagnotto, M. E., Vilaythong, A. J., Thwin, M. T., Noebels, J. L., Baraban, S. C., & Rubenstein, J. L. R. (2005a). Mice lacking Dlx1 show subtype-specific loss of interneurons, reduced inhibition and epilepsy. *Nature Neuroscience*, *8*(8), 1059–1068. https://doi.org/10.1038/NN1499

Depew, M. J., Liu, J. K., Long, J. E., Presley, R., Meneses, J. J., Pedersen, R. A., & Rubenstein, J. L. R. (1999). Dlx5 regulates regional development of the branchial arches and sensory

capsules. *Development (Cambridge, England)*, *126*(17), 3831–3846. https://doi.org/10.1242/DEV.126.17.3831

D'Gama, P. P., Jeong, I., Nygård, A. M., Trinh, A. T., Yaksi, E., & Jurisch-Yaksi, N. (2024). Ciliogenesis defects after neurulation impact brain development and neuronal activity in larval zebrafish. *IScience*, *27*(6), 110078. https://doi.org/10.1016/J.ISCI.2024.110078

Druga, R., Salaj, M., & Al-Redouan, A. (2023). Parvalbumin - Positive Neurons in the Neocortex: A Review. *Physiological Research*, *72*(Suppl 2), S173. https://doi.org/10.33549/PHYSIOLRES.935005

Ellies, D. L., Stock, D. W., Hatch, G., Giroux, G., Weiss, K. M., & Ekker, M. (1997). Relationship between the genomic organization and the overlapping embryonic expression patterns of the zebrafish dlx genes. *Genomics*, *45*(3), 580–590. https://doi.org/10.1006/GENO.1997.4978

Farrell, J. A., Wang, Y., Riesenfeld, S. J., Shekhar, K., Regev, A., & Schier, A. F. (2018). Single-cell reconstruction of developmental trajectories during zebrafish embryogenesis. *Science (New York, N.Y.)*, *360*(6392). https://doi.org/10.1126/SCIENCE.AAR3131

Fazel Darbandi, S., Poitras, L., Monis, S., Lindtner, S., Yu, M., Hatch, G., Rubenstein, J. L., & Ekker, M. (2016). Functional consequences of I56ii Dlx enhancer deletion in the developing mouse forebrain. *Developmental Biology*, *420*(1), 32–42. https://doi.org/10.1016/J.YDBIO.2016.10.015

Friedberg, F. (2005). Parvalbumin isoforms in zebrafish. *Molecular Biology Reports*, *32*(3), 167–175. https://doi.org/10.1007/S11033-005-2334-4

Ganguly, K., Schinder, A. F., Wong, S. T., & Poo, M. ming. (2001). GABA itself promotes the developmental switch of neuronal GABAergic responses from excitation to inhibition. *Cell*, *105*(4), 521–532. https://doi.org/10.1016/S0092-8674(01)00341-5

Ghanem, N., Jarinova, O., Amores, A., Long, Q., Hatch, G., Park, B. K., Rubenstein, J. L. R., & Ekker, M. (2003a). Regulatory Roles of Conserved Intergenic Domains in Vertebrate Dlx Bigene Clusters. *Genome Research*, *13*(4), 533. https://doi.org/10.1101/GR.716103

Gulyás, A. I., Hájos, N., & Freund, T. F. (1996). Interneurons Containing Calretinin Are Specialized to Control Other Interneurons in the Rat Hippocampus. *The Journal of Neuroscience*, *16*(10), 3397. https://doi.org/10.1523/JNEUROSCI.16-10-03397.1996

Guo, Z., Su, Y., Huang, W., Yao, X. S., Hong, Y., Gordin, A., Nguyen, H. N., Wen, Z., Ringeling, F. R., Chen, G., Li, S., Lu, L., Xia, M., Zheng, W., Sawa, A., Chen, G., Christian, K. M., Song, H., & Ming, G. (2024). GABAergic neuron dysregulation in a human neurodevelopmental model

for major psychiatric disorders. *BioRxiv : The Preprint Server for Biology*. https://doi.org/10.1101/2024.09.23.614564

Howe, K., Clark, M. D., Torroja, C. F., Torrance, J., Berthelot, C., Muffato, M., Collins, J. E., Humphray, S., McLaren, K., Matthews, L., McLaren, S., Sealy, I., Caccamo, M., Churcher, C., Scott, C., Barrett, J. C., Koch, R., Rauch, G. J., White, S., … Stemple, D. L. (2013). The zebrafish reference genome sequence and its relationship to the human genome. *Nature*, *496*(7446), 498–503. https://doi.org/10.1038/NATURE12111

Hu, H., Gan, J., & Jonas, P. (n.d.). *Fast-spiking, parvalbumin + GABAergic interneurons: From cellular design to microcircuit function*. Retrieved March 15, 2026, from https://www.science.org

Kenney, J. W., Steadman, P. E., Young, O., Shi, M. T., Polanco, M., Dubaishi, S., Covert, K., Mueller, T., & Frankland, P. W. (2021). A 3d adult zebrafish brain atlas (Azba) for the digital age. *ELife*, *10*. https://doi.org/10.7554/ELIFE.69988

Kizil, C., Kaslin, J., Kroehne, V., & Brand, M. (2012). Adult neurogenesis and brain regeneration in zebrafish. *Developmental Neurobiology*, *72*(3), 429–461. https://doi.org/10.1002/DNEU.20918

Klausberger, T., & Somogyi, P. (2008). Neuronal Diversity and Temporal Dynamics: The Unity of Hippocampal Circuit Operations. *Science (New York, N.Y.)*, *321*(5885), 53. https://doi.org/10.1126/SCIENCE.1149381

Le, T. N., Zhou, Q. P., Cobos, I., Zhang, S., Zagozewski, J., Japoni, S., Vriend, J., Parkinson, T., Du, G., Rubenstein, J. L., & Eisenstat, D. D. (2017). GABAergic Interneuron Differentiation in the Basal Forebrain Is Mediated through Direct Regulation of Glutamic Acid Decarboxylase Isoforms by Dlx Homeobox Transcription Factors. *The Journal of Neuroscience : The Official Journal of the Society for Neuroscience*, *37*(36), 8816–8829. https://doi.org/10.1523/JNEUROSCI.2125-16.2017

Lee, S., Kruglikov, I., Huang, Z. J., Fishell, G., & Rudy, B. (2013). A disinhibitory circuit mediates motor integration in the somatosensory cortex. *Nature Neuroscience*, *16*(11), 1662–1670. https://doi.org/10.1038/NN.3544

Lindsey, B. W., Douek, A. M., Loosli, F., & Kaslin, J. (2018). A whole brain staining, embedding, and clearing pipeline for adult zebrafish to visualize cell proliferation and morphology in 3-dimensions. *Frontiers in Neuroscience*, *11*(JAN), 750. https://doi.org/10.3389/FNINS.2017.00750/FULL

Liu, J. K. (n.d.). Dlx genes encode DNA-binding proteins that are expressed in an overlapping and sequential pattern during basal ganglia differentiation. *Developmental Dynamics*, *210*(4).

Retrieved March 27, 2026, from https://resolver.scholarsportal.info/resolve/10588388/v210i0004/498_dgedptspdbgd.xml

Long, J. E., Garel, S., Alvarez-Dolado, M., Yoshikawa, K., Osumi, N., Alvarez-Buylla, A., & Rubenstein, J. L. R. (2007). Dlx-dependent and -independent regulation of olfactory bulb interneuron differentiation. *The Journal of Neuroscience : The Official Journal of the Society for Neuroscience*, *27*(12), 3230–3243. https://doi.org/10.1523/JNEUROSCI.5265-06.2007

Long, J. E., Swan, C., Liang, W. S., Cobos, I., Potter, G. B., & Rubenstein, J. L. R. (2009). Dlx1&2 and Mash1 transcription factors control striatal patterning and differentiation through parallel and overlapping pathways. *The Journal of Comparative Neurology*, *512*(4), 556–572. https://doi.org/10.1002/CNE.21854

MacDonald, R. B., Pollack, J. N., Debiais-Thibaud, M., Heude, E., Coffin Talbot, J., & Ekker, M. (2013). The ascl1a and dlx genes have a regulatory role in the development of GABAergic interneurons in the zebrafish diencephalon. *Developmental Biology*, *381*(1), 276–285. https://doi.org/10.1016/J.YDBIO.2013.05.025

MacKenzie, R. K., Sankar, P. R., & Bendall, A. J. (2019). Dlx5 and Dlx6 can antagonize cell division at the G1/S checkpoint. *BMC Molecular and Cell Biology*, *20*(1). https://doi.org/10.1186/S12860-019-0191-6

Marín, O. (2012). Interneuron dysfunction in psychiatric disorders. *Nature Reviews. Neuroscience*, *13*(2), 107–120. https://doi.org/10.1038/NRN3155

Mendes, H. W., Taktek, M., Duret, T., & Ekker, M. (2020a). Expression of dlx genes in the normal and regenerating brain of adult zebrafish. *PLOS ONE*, *15*(6), e0229549. https://doi.org/10.1371/JOURNAL.PONE.0229549

Merlo, G. R., Zerega, B., Paleari, L., Trombino, S., Mantero, S., & Levi, G. (2000). Multiple functions of Dlx genes. *International Journal of Developmental Biology*, *44*(6), 619–626. https://doi.org/10.1387/IJDB.11061425

Morasso, M. I., & Radoja, N. (2005). Dlx genes, p63, and ectodermal dysplasias. *Birth Defects Research. Part C, Embryo Today : Reviews*, *75*(3), 163–171. https://doi.org/10.1002/BDRC.20047

Panganiban, G., Irvine, S. M., Lowe, C., Roehl, H., Corley, L. S., Sherbon, B., Grenier, J. K., Fallon, J. F., Kimble, J., Walker, M., Wray, G. A., Swalla, B. J., Martindale, M. Q., & Carroll, S. B. (1997). The origin and evolution of animal appendages. *Proceedings of the National Academy of Sciences of the United States of America*, *94*(10), 5162–5166. https://doi.org/10.1073/PNAS.94.10.5162/ASSET/7B9D41CB-B425-49F8-93C1-0BC2ADD67F2D/ASSETS/GRAPHIC/PQ0970662004.JPEG

Panganiban, G., & Rubenstein, J. L. R. (2002). Developmental functions of the Distal-less/Dlx homeobox genes. *Development (Cambridge, England)*, *129*(19), 4371–4386. https://doi.org/10.1242/DEV.129.19.4371

Pfeffer, C. K., Xue, M., He, M., Huang, Z. J., & Scanziani, M. (2013). Inhibition of Inhibition in Visual Cortex: The Logic of Connections Between Molecularly Distinct Interneurons. *Nature Neuroscience*, *16*(8), 1068. https://doi.org/10.1038/NN.3446

Pla, R., Stanco, A., Howard, M. A., Rubin, A. N., Vogt, D., Mortimer, N., Cobos, I., Potter, G. B., Lindtner, S., Price, J. D., Nord, A. S., Visel, A., Schreiner, C. E., Baraban, S. C., Rowitch, D. H., & Rubenstein, J. L. R. (2017). Dlx1 and Dlx2 Promote Interneuron GABA Synthesis, Synaptogenesis, and Dendritogenesis. *Cerebral Cortex (New York, NY)*, *28*(11), 3797. https://doi.org/10.1093/CERCOR/BHX241

Pla, R., Stanco, A., Howard, M. A., Rubin, A. N., Vogt, D., Mortimer, N., Cobos, I., Potter, G. B., Lindtner, S., Price, J. D., Nord, A. S., Visel, A., Schreiner, C. E., Baraban, S. C., Rowitch, D. H., & Rubenstein, J. L. R. (2018). Dlx1 and Dlx2 Promote Interneuron GABA Synthesis, Synaptogenesis, and Dendritogenesis. *Cerebral Cortex*, *28*(11), 3797–3815. https://doi.org/10.1093/CERCOR/BHX241

Pouille, F., & Scanziani, M. (2001). Enforcement of temporal fidelity in pyramidal cells by somatic feed-forward inhibition. *Science (New York, N.Y.)*, *293*(5532), 1159–1163. https://doi.org/10.1126/SCIENCE.1060342

Ramaswamy, M., Cheng, R. K., & Jesuthasan, S. (2020). Identification of GABAergic neurons innervating the zebrafish lateral habenula. *The European Journal of Neuroscience*, *52*(8), 3918. https://doi.org/10.1111/EJN.14843

Rubenstein, J. L., Nord, A. S., & Ekker, M. (2024). DLX genes and proteins in mammalian forebrain development. *Development (Cambridge, England)*, *151*(11), dev202684. https://doi.org/10.1242/DEV.202684

Rudy, B., Fishell, G., Lee, S. H., & Hjerling-Leffler, J. (2011). Three groups of interneurons account for nearly 100% of neocortical GABAergic neurons. *Developmental Neurobiology*, *71*(1), 45–61. https://doi.org/10.1002/DNEU.20853

Solek, C. M., Feng, S., Perin, S., Weinschutz Mendes, H., & Ekker, M. (2017). Lineage tracing of dlx1a/2a and dlx5a/6a expressing cells in the developing zebrafish brain. *Developmental Biology*, *427*(1), 131–147. https://doi.org/10.1016/J.YDBIO.2017.04.019

Stock, D. W., Ellies, D. L., Zhao, Z., Ekker, M., Ruddle, F. H., & Weiss, K. M. (1996). The evolution of the vertebrate Dlx gene family. *Proceedings of the National Academy of Sciences of the*

United States of America, *93*(20), 10858–10863. https://doi.org/10.1073/PNAS.93.20.10858

Sur, A., Wang, Y., Capar, P., Margolin, G., Prochaska, M. K., & Farrell, J. A. (2023). Single-cell analysis of shared signatures and transcriptional diversity during zebrafish development. *Developmental Cell*, *58*(24), 3028-3047.e12. https://doi.org/10.1016/J.DEVCEL.2023.11.001

Taylor, J. S., Braasch, I., Frickey, T., Meyer, A., & Van de Peer, Y. (2003). Genome duplication, a trait shared by 22000 species of ray-finned fish. *Genome Research*, *13*(3), 382–390. https://doi.org/10.1101/GR.640303

Tremblay, R., Lee, S., & Rudy, B. (2016). GABAergic Interneurons in the Neocortex: From Cellular Properties to Circuits. *Neuron*, *91*(2), 260–292. https://doi.org/10.1016/J.NEURON.2016.06.033

Urban-Ciecko, J., & Barth, A. L. (2016). Somatostatin-expressing neurons in cortical networks. *Nature Reviews. Neuroscience*, *17*(7), 401. https://doi.org/10.1038/NRN.2016.53

Vanessa Becerra-Hernández, L., Casanova, M. F., & Buriticá, E. (2025). Cortical calretinin-positive neurons: Functional and ontogenetic characteristics and their relationship to brain pathologies. *Brain Research*, *1846*, 149285. https://doi.org/10.1016/J.BRAINRES.2024.149285

Wang, K., Yu, Y., Xu, Y., Yue, Y., Zhao, F., Feng, W., Duan, Y., Duan, W., Yue, J., Liao, Z., Fei, P., Sun, H., & Xiong, B. (2023). TSA-PACT: a method for tissue clearing and immunofluorescence staining on zebrafish brain with improved sensitivity, specificity and stability. *Cell & Bioscience*, *13*(1), 97. https://doi.org/10.1186/S13578-023-01043-1

Wang, Y., Toledo-Rodriguez, M., Gupta, A., Wu, C., Silberberg, G., Luo, J., & Markram, H. (2004). Anatomical, physiological and molecular properties of Martinotti cells in the somatosensory cortex of the juvenile rat. *The Journal of Physiology*, *561*(Pt 1), 65. https://doi.org/10.1113/JPHYSIOL.2004.073353

Wonders, C. P., & Anderson, S. A. (2006). The origin and specification of cortical interneurons. *Nature Reviews. Neuroscience*, *7*(9), 687–696. https://doi.org/10.1038/NRN1954

Yu, E. P. Y., Perin, S., Saxena, V., & Ekker, M. (2021). Novel cross-regulation interactions between dlx genes in larval zebrafish. *Gene*, *801*, 145848. https://doi.org/10.1016/J.GENE.2021.145848

Zerucha, T., & Ekker, M. (2011). Distal-less-related homeobox genes of vertebrates: Evolution, function, and regulation. *Https://Doi.Org/10.1139/O00-066*, *78*(5), 593–601. https://doi.org/10.1139/O00-066

Zerucha, T., Stühmer, T., Hatch, G., Park, B. K., Long, Q., Yu, G., Gambarotta, A., Schultz, J. R., Rubenstein, J. L. R., & Ekker, M. (2000). A Highly Conserved Enhancer in the Dlx5/Dlx6Intergenic Region is the Site of Cross-Regulatory Interactions betweenDlx Genes in the Embryonic Forebrain. *The Journal of Neuroscience*, *20*(2), 709. https://doi.org/10.1523/JNEUROSCI.20-02-00709.2000